↑ ↑ ↑ ↑ ↑ ↑ →→→ ↓ ↓ ↓ ↓ ↓ ↓ ↓

Two-Dimensional Nanomagnetics

2014

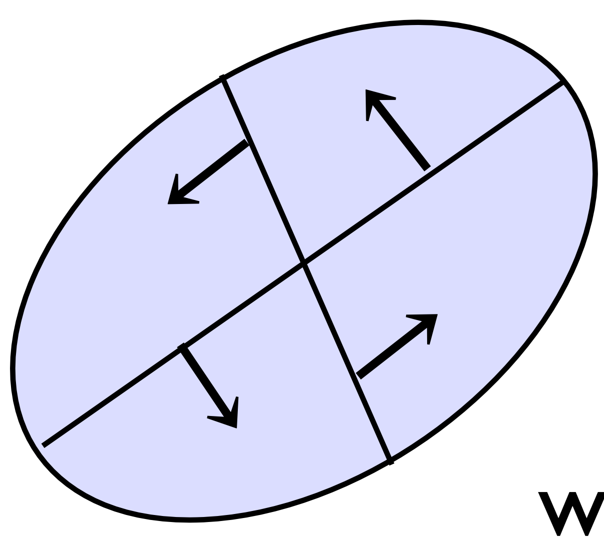

Gary Wysin
Kansas State University
Manhattan, Kansas, U.S.A.

wysin@phys.ksu.edu
www.phys.ksu.edu/personal/wysin

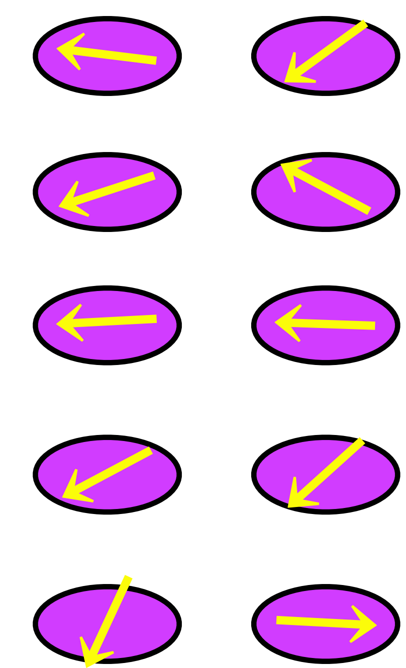

Magnetic Nano-Islands

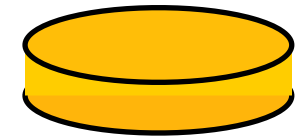

Approx. 50 nm - 5 μm wide but only 10 nm thick.
Individual & in arrays, high-permeability soft magnetic materials.
Grown with techniques of epitaxy & lithography on a non-magnetic substrate.
Form arrays of particles that can interact with each other or applied fields.

Primary physics effects -

- magnetostatics controlled by island geometry.
- discrete energy states for data storage.
- spintronics controlled by current injection.
- magnetic oscillators controlled by applied fields.
- frustration in ordered arrays of islands (spin-ice).

Several principle states of a nano-island:

(1) quasi-single domain; (2) vortex; (3) multi-domains & domain walls.

~ increasing size ~

Magnetic nano-island applications

☛ memory elements, signal processing

☛ non-volatile data storage (magnetic ram)

☛ use in sensors of (giant) magneto-resistance (GMR)

☛ integration into spintronics (switching between states via spin polarized currents.)

⊙ a one-vortex state with small stray magnetic field.

Three things to be studied:

1) Vortices. The static and dynamic properties of single vortices. They behave very much as particles with charges.

2) Magnetostatic anisotropy of the islands themselves. Also known as shape anisotropy because it depends mostly on the surfaces.

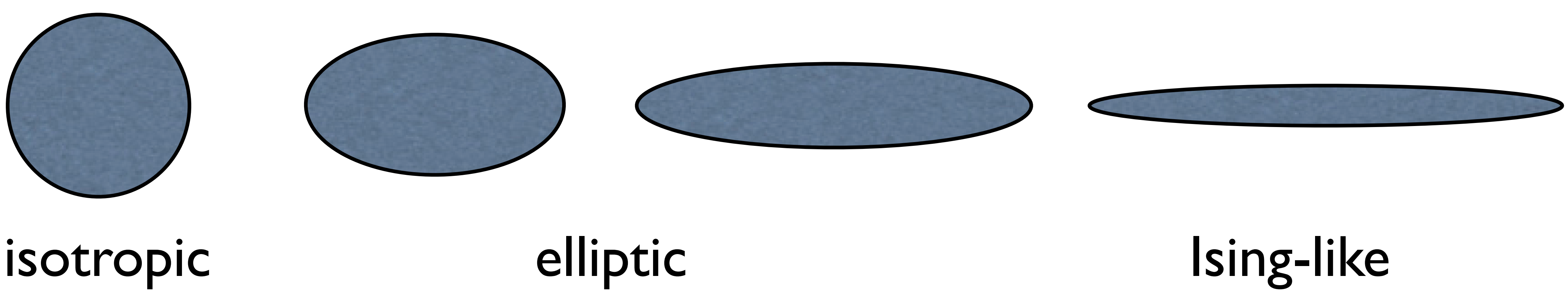

3) Spin-ices. Especially for elongated islands with Ising-like states, interactions within their arrays, that lead to frustrated statics and dynamics.

Magnetostatics - For $L_x \times L_y \times L_z$ elliptical islands.

Basic theory of magnetostatic energy and demagnetization:

Maxwell eqns, for H_M caused by M: $\vec{\nabla}\cdot\vec{B}=0, \quad \vec{B}=\mu_0(\vec{H}_M+\vec{M}).$

The magnetostatic energy is: $$E_M=-\frac{1}{2}\mu_0\int \mathrm{d}V\ \vec{M}\cdot\vec{H}_M.$$

The demagnetization field solves: $\vec{\nabla}\cdot\vec{H}_M=-\vec{\nabla}\cdot\vec{M}.$ $\boxed{\rho_M=-\vec{\nabla}\cdot\vec{M}.}$

Put: $\boxed{\vec{H}_M=-\vec{\nabla}\Phi_M}$ $\Rightarrow$

$$\nabla^2\Phi_M=-\rho_M.$$

Poisson's equation.

Magnetization M determines an effective surface charge density:

$$\boxed{\sigma_M = \vec{M} \cdot \hat{n},}$$

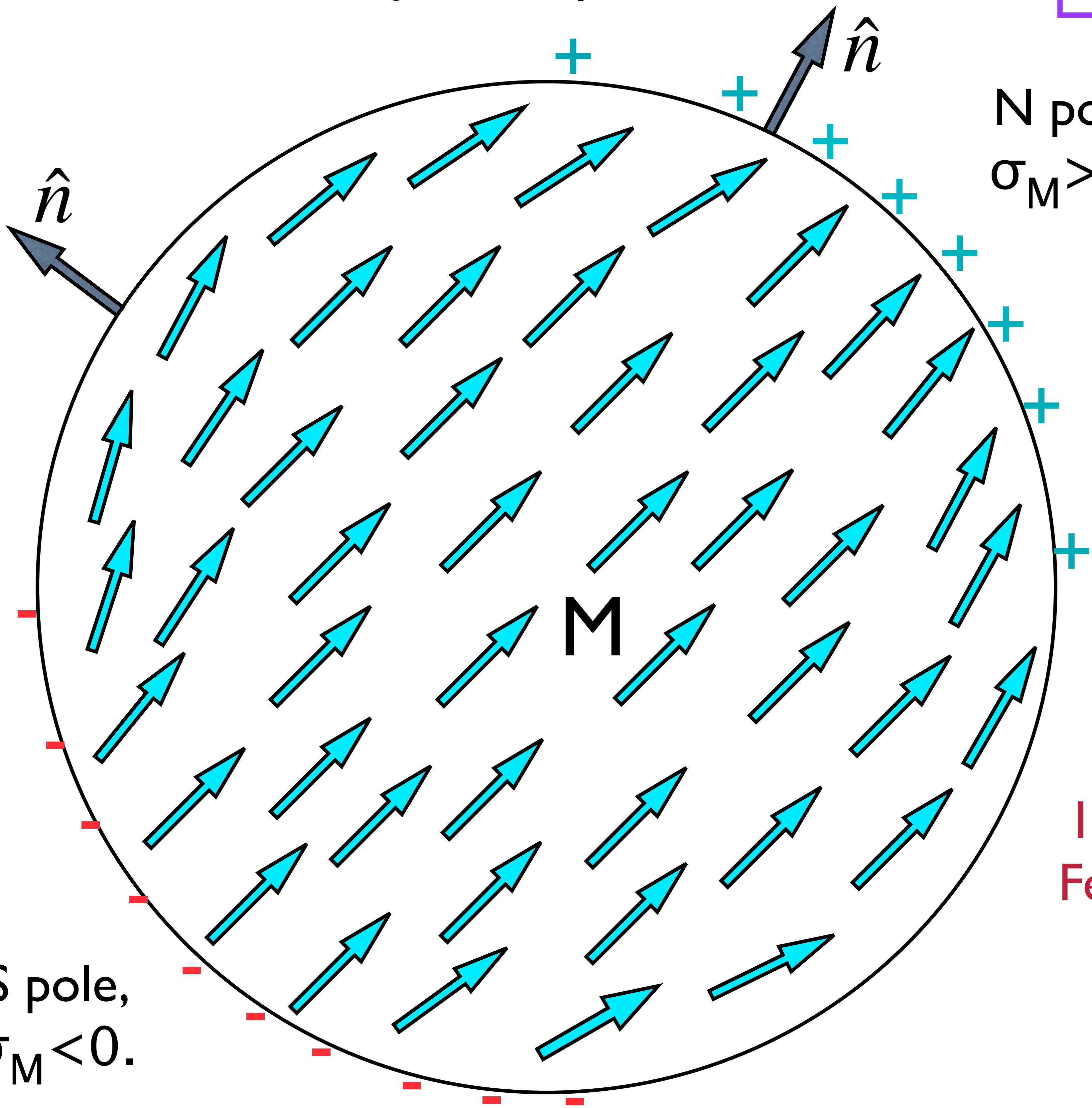

N pole, $\sigma_M > 0$.

S pole, $\sigma_M < 0$.

The poles involve extra energy.

1) Quasi-single-domain. Ferromagnetic exchange energy is small.

(2) Vortex state

Very little magnetic surface charge density.
Stable only above a minimum radius

$$\sigma_M = \vec{M} \cdot \hat{n},$$

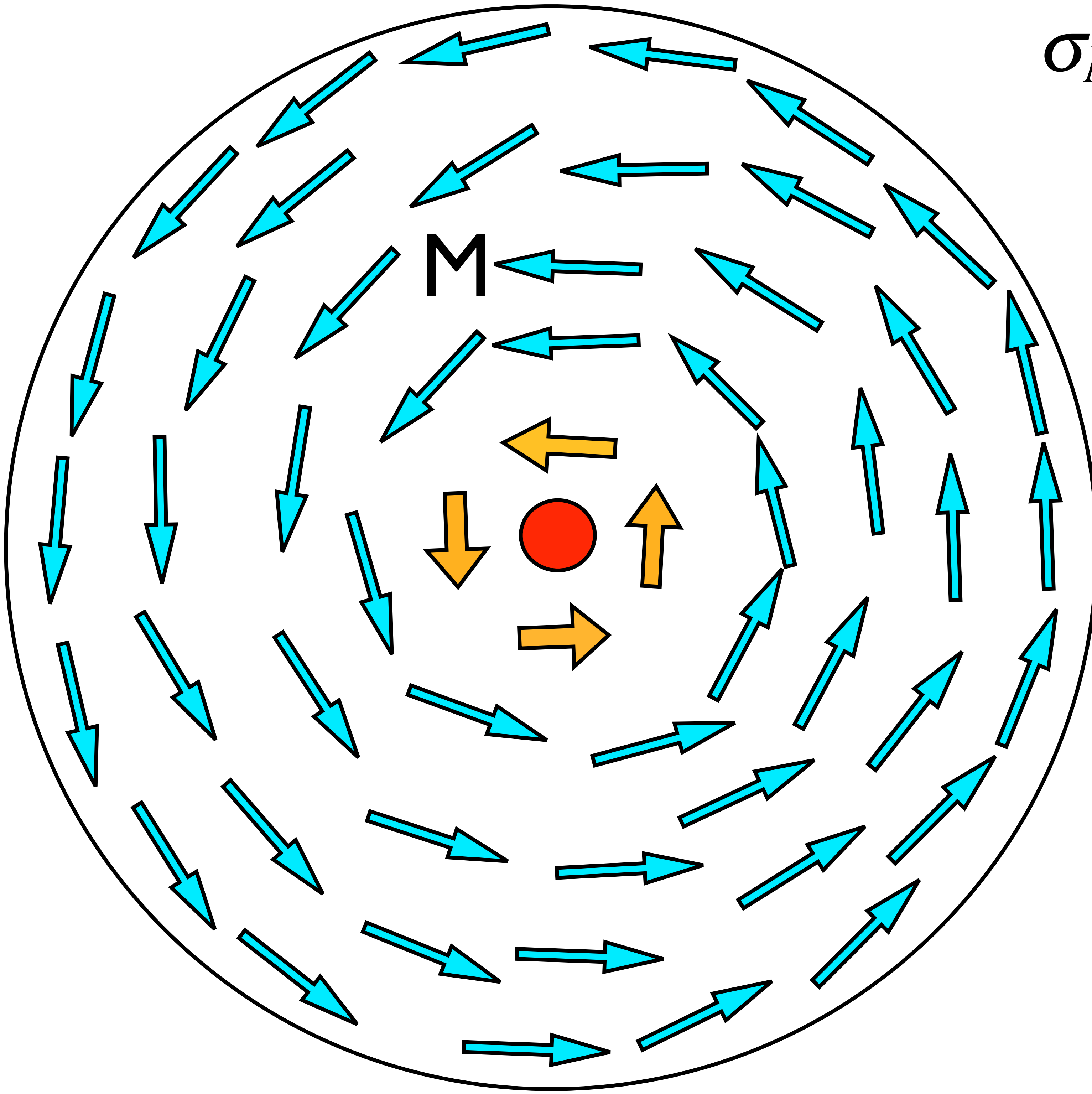

Has poles ($\sigma_M = \pm M_z$) only in the core.

Their energy is small.

Now the energy of FM exchange is greater.

Elongated islands -
Highly anisotropic.

Ising-like interaction
and behavior.

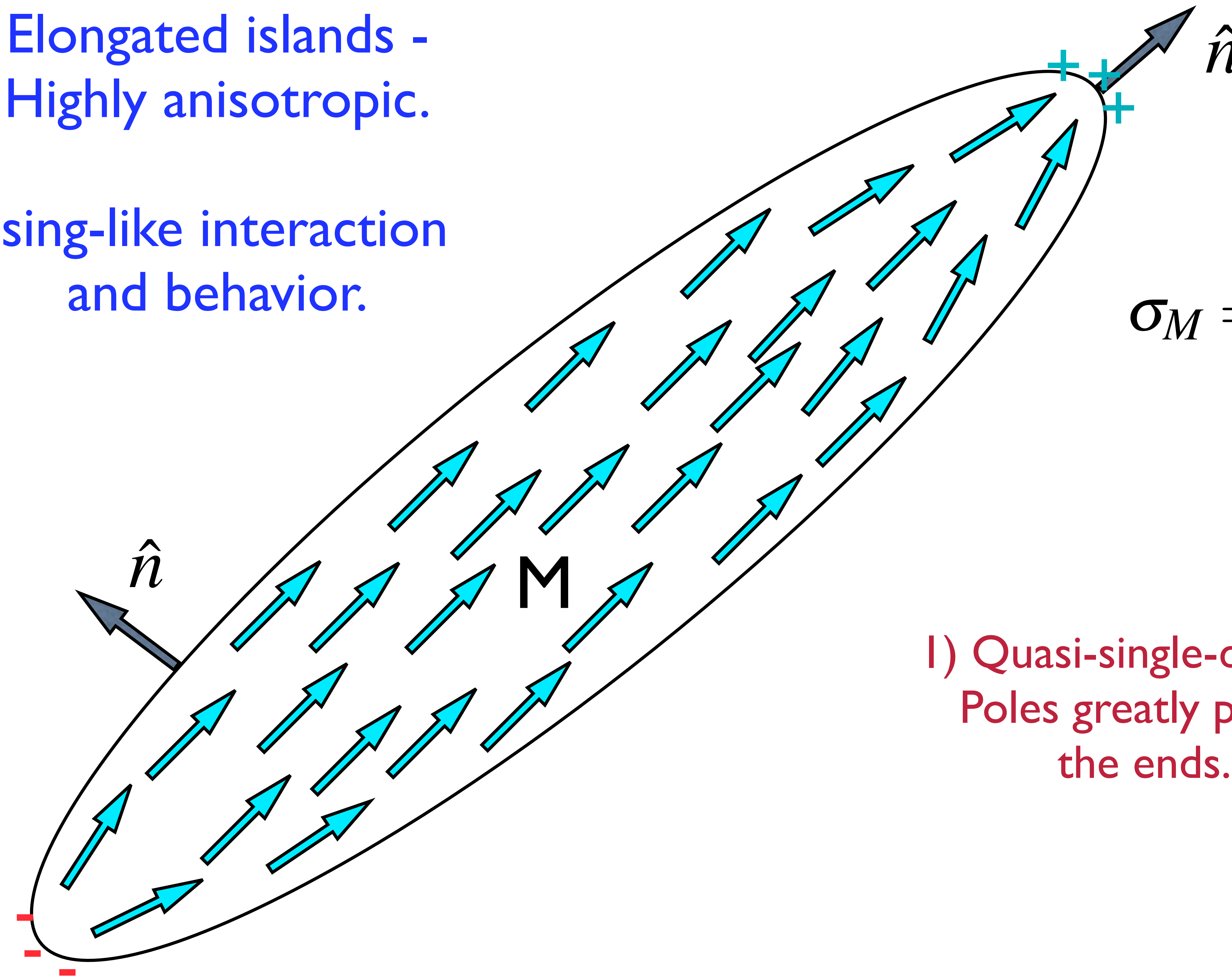

$$\sigma_M = \vec{M} \cdot \hat{n},$$

1) Quasi-single-domain.
Poles greatly prefer
the ends.

Micromagnetics. A technique for studying a continuous system.

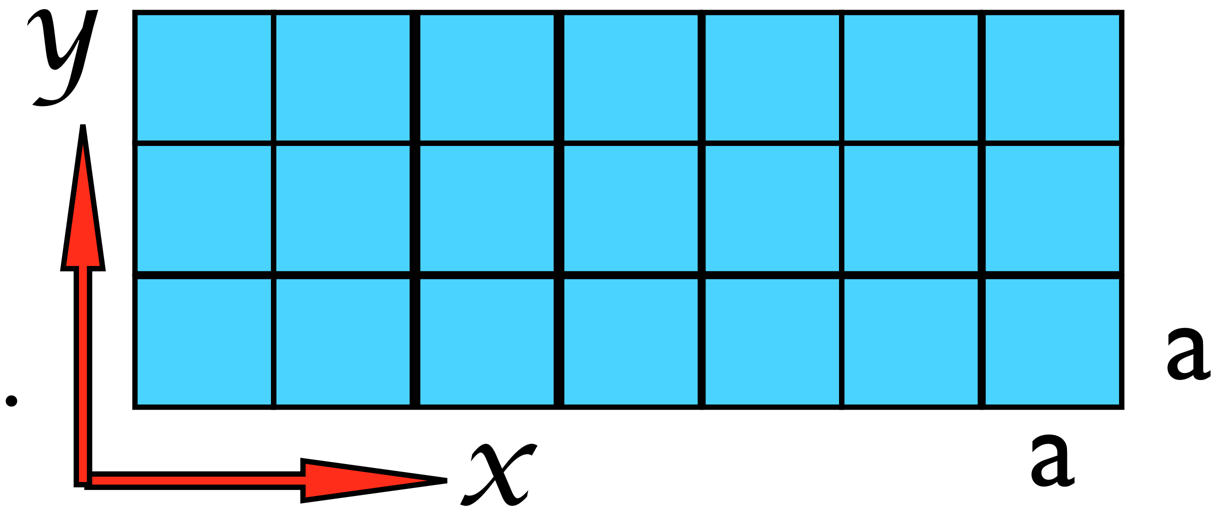

Each cell contains a magnetic dipole:

$$\hat{m} = \vec{M}/M_S.$$

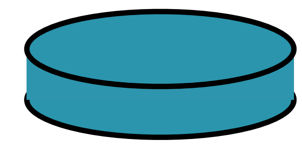

- Model for a cylindrical islands, radii R_A, R_B, height L.

- Divide the sample into cells of size a x a x L.

- Assume that the magnetization is saturated (M_S) inside each cell: $|m|=1$. Only the directions vary between cells.

- The cells interact as dipoles, with exchange energy between neighbors & with the demagnetization field.

Micromagnetics

Hamiltonian: $\boxed{\mathcal{H} = \mathcal{H}_{\mathrm{ex}} + \mathcal{H}_{\mathrm{demag}} + \mathcal{H}_{\mathrm{B}}}$

exchange: $$\mathcal{H}_{\mathrm{ex}} = A \int dV \ \nabla \hat{m} \cdot \nabla \hat{m},$$

magnetostatic (demagnetization): $$\mathcal{H}_{\mathrm{dd}} = \mathcal{H}_{\mathrm{demag}} = -\frac{1}{2}\mu_0 \int \ dV \ \vec{H}_M \cdot \vec{M}$$

applied field: $$\mathcal{H}_B = -\mu_0 \int \ dV \ \vec{H}_{\mathrm{ext}} \cdot \vec{M}$$

Statics: minimize the energy $\Rightarrow$ stable configurations.
Dynamics: equation of motion $\Rightarrow$ periodic configurations.

Difficulties:

(i) Calculating the demagnetization field H_M;

(ii) Enforcing a desired initial position, X, of a vortex $\Rightarrow$ E(X).

Scale energies by the exchange between cells:

$$J_{\rm cell} = \frac{2Av_{\rm cell}}{a^2} = 2AL.$$

"magnetic exchange length"

$$\lambda_{\rm ex} = \sqrt{\frac{2A}{\mu_0 M_S^2}}$$

demag. field:

$$\vec{H}_M = M_S \tilde{H}_M$$

Hamiltonian on the grid of cells:

$$\mathcal{H}_{\rm mm} = -J_{\rm cell} \left\{ \sum_{(i,j)} \hat{m}_i \cdot \hat{m}_j + \left(\frac{a}{\lambda_{\rm ex}}\right)^2 \sum_i \left(\tilde{H}_{\rm ext} + \frac{1}{2}\tilde{H}_M \right) \cdot \hat{m}_i \right\}$$

Need $\left(\frac{a}{\lambda_{\rm ex}}\right)^2$ less than 1 for reliable solutions.

(cells smaller than exchange length)

Finding the demagnetization field via Green/FFT approach.

The magnetostatics problem has no free currents:

$$-\tilde{\nabla}^2\tilde{\Phi} = \tilde{\rho} \qquad \tilde{\rho} \equiv -\tilde{\nabla}\cdot\hat{m} \qquad \tilde{H}_M = -\tilde{\nabla}\tilde{\Phi}$$

use Green's function solution:

$$\tilde{\Phi}(\vec{r}) = \int d^3r'\ G(\vec{r},\vec{r}\,')\,\tilde{\rho}(\vec{r}\,') \qquad G(\vec{r},\vec{r}\,') = \frac{1}{4\pi|\vec{r}-\vec{r}\,'|}$$

specialize to a thin cylinder (2D) geometry: $\tilde{r} \equiv (x, y)$

$$\tilde{H}_z(\tilde{r}) = \int d^2\tilde{r}\,'\ G_z(\tilde{r}-\tilde{r}\,')\ m_z(\tilde{r}\,')$$

$$\tilde{H}_{xy}(\tilde{r}) = \int d^2\tilde{r}\,'\ \vec{G}_{xy}(\tilde{r}-\tilde{r}\,')\ \tilde{\rho}(\tilde{r}\,')$$

$$G_z(\tilde{r}) = \frac{1}{2\pi L}\left[\frac{1}{\sqrt{\tilde{r}^2+L^2}} - \frac{1}{|\tilde{r}|}\right]$$

$$\vec{G}_{xy}(\tilde{r}) = \frac{1}{2\pi L}\left[\sqrt{1+\left(\frac{L}{\tilde{r}}\right)^2} - 1\right]\hat{e}_{\tilde{r}}$$

Other details.

The magnetic charge densities depend on the present magnetic configuration, such as:

$$\tilde{\rho}_0^{\text{vol}} = \frac{q_M^{\text{vol}}}{La^2} = -\frac{1}{2a}\left[m_1^x - m_3^x + m_2^y - m_4^y\right]$$

$$\tilde{\rho}_0^{\text{sur}} = \frac{q_M^{\text{sur}}}{La^2} = \sum_{\text{cell edges}} \frac{1}{2a}\hat{m}_0 \cdot \hat{n}_{\text{edge}}$$

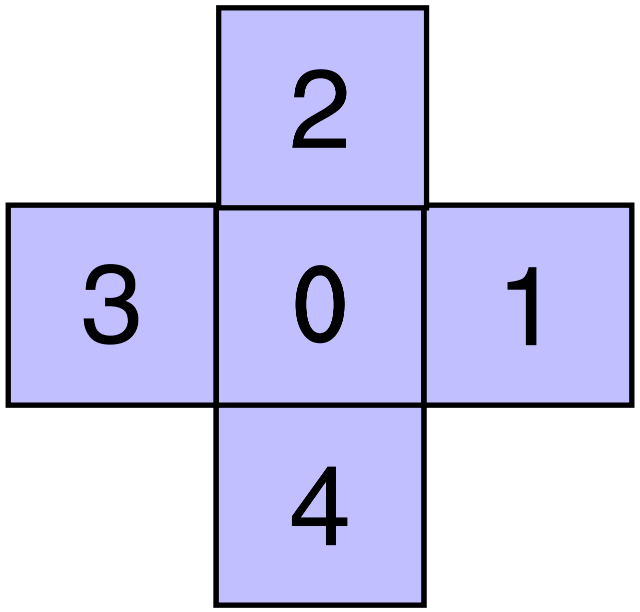

Convolutions are evaluated using fast fourier transforms.

Use zero padding to avoid the wrap-around problem:
FFT grid is 2X larger than original system to avoid false copies.

The solution for demagnetization field is that for an island isolated from others.

1) Vortices: Particle-like properties

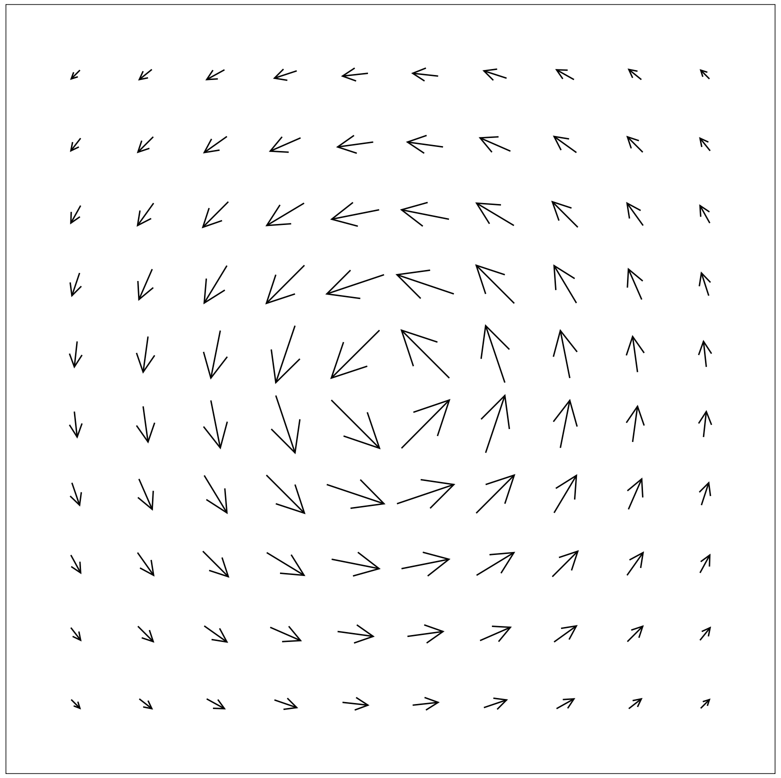

M(r)

“vorticity charge”

$$q = \frac{1}{2\pi} \oint \vec{\nabla}\phi \cdot d\vec{r} = 0, \pm 1$$

circulation or *curling*

$-1 \leq C \leq +1$

$$C = \frac{1}{N} \sum_i \hat{\sigma}_i \cdot \hat{\phi}_i \qquad \hat{\sigma}_i = \vec{\mu}_i / \mu.$$

polarization

$p = m_z = \pm 1$ in the nucleus

“topological charge = gyrovector”

$G = 2\pi pq =$ solid angle mapped out by all the spins

Vortex, q=+1, p=+1
R=30nm, L=8nm

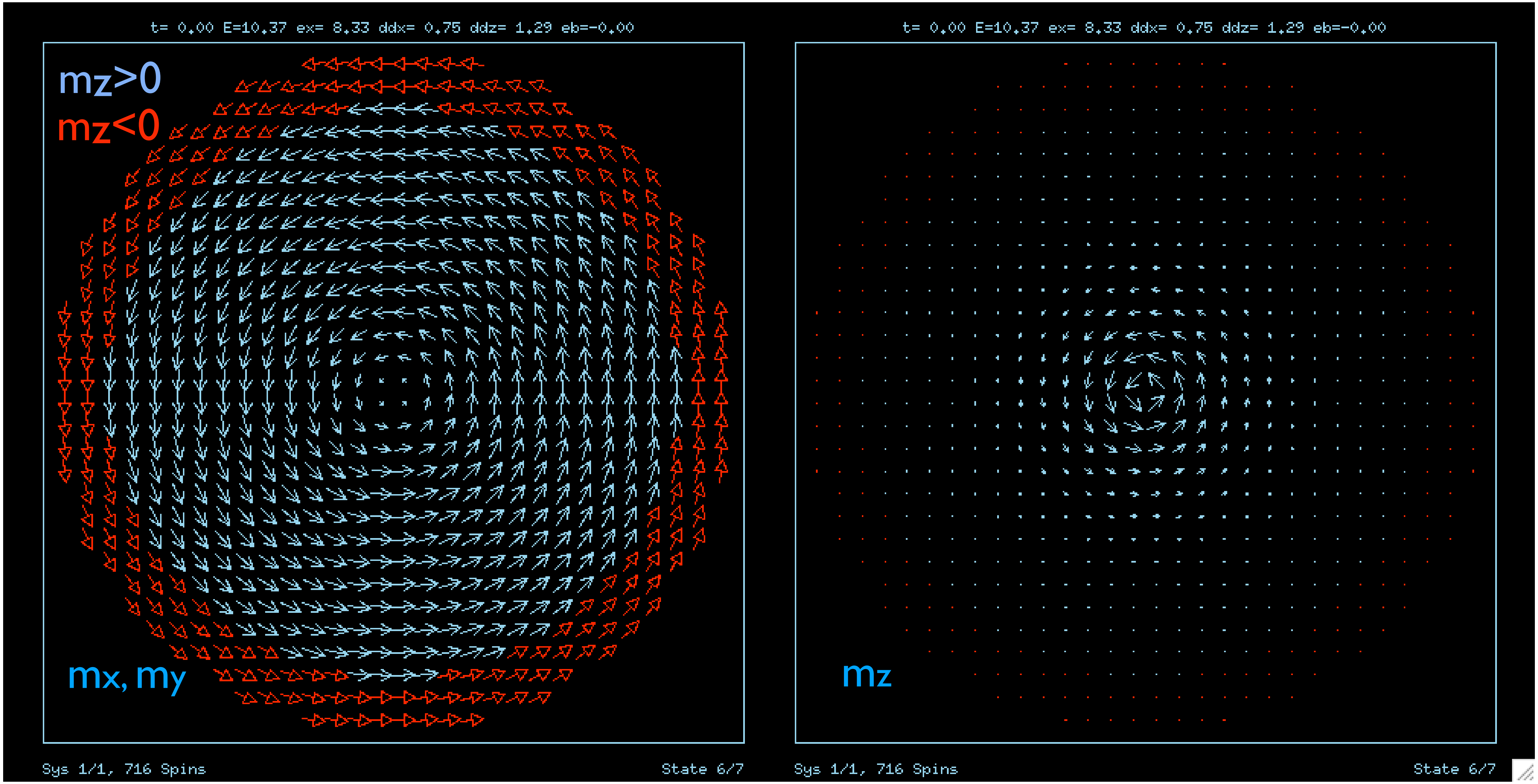

Gyrotropic movement

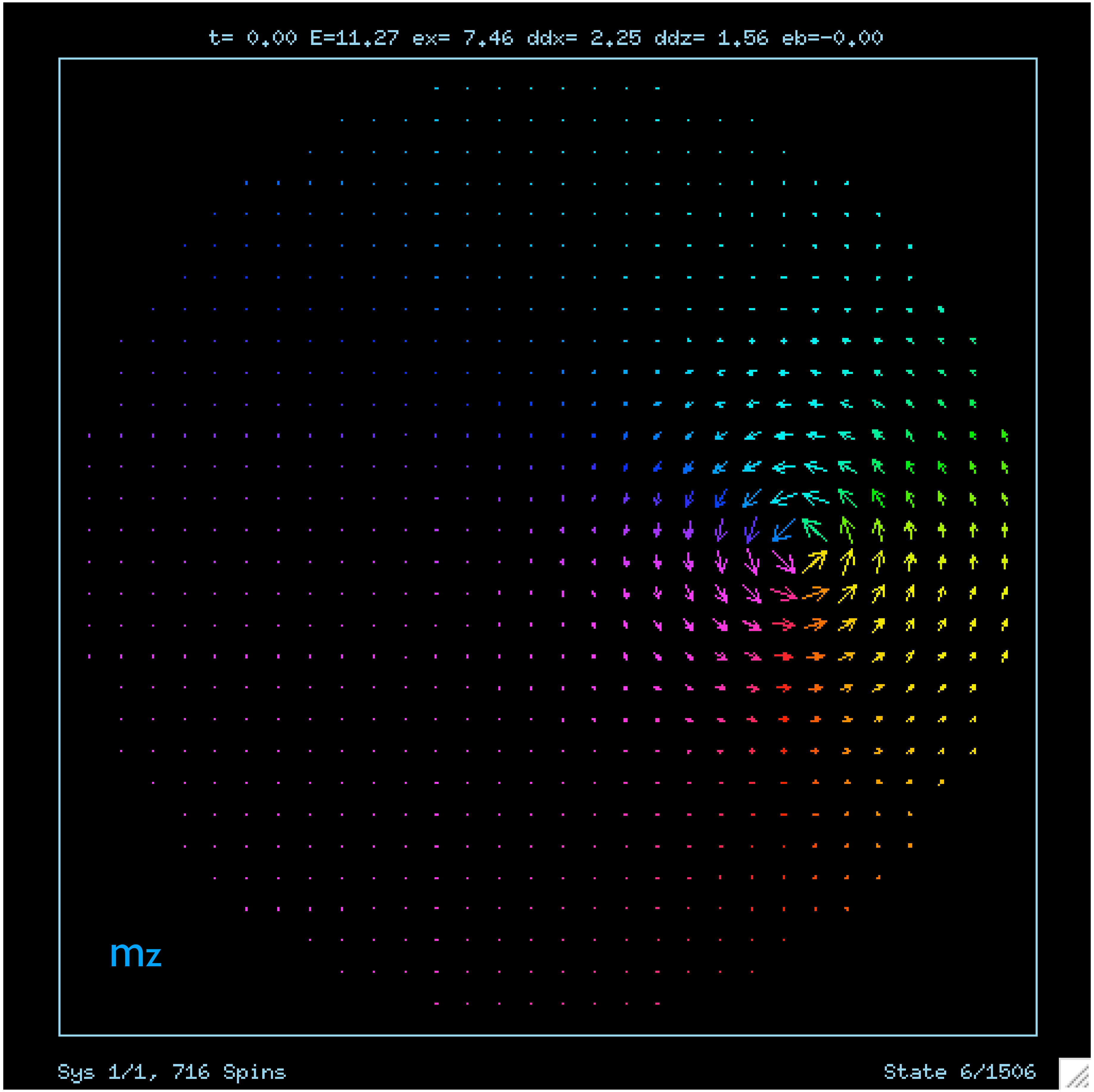

R=30 nm,
L=10 nm,
cells a=2.0 nm

Vortex,
q=+1, p=+1

The arrows are proportional to Mz, out of the plane.

time unit = 0.75 ps

Example. Total energy of a vortex, $E(x_0) \approx \frac{1}{2} k_F x_0^2$

$a = 2.0$ nm, $\lambda_{ex} = 5.3$ nm, $\boxed{L = 12 \text{ nm},}$ $R = 40, 80, 120$ nm

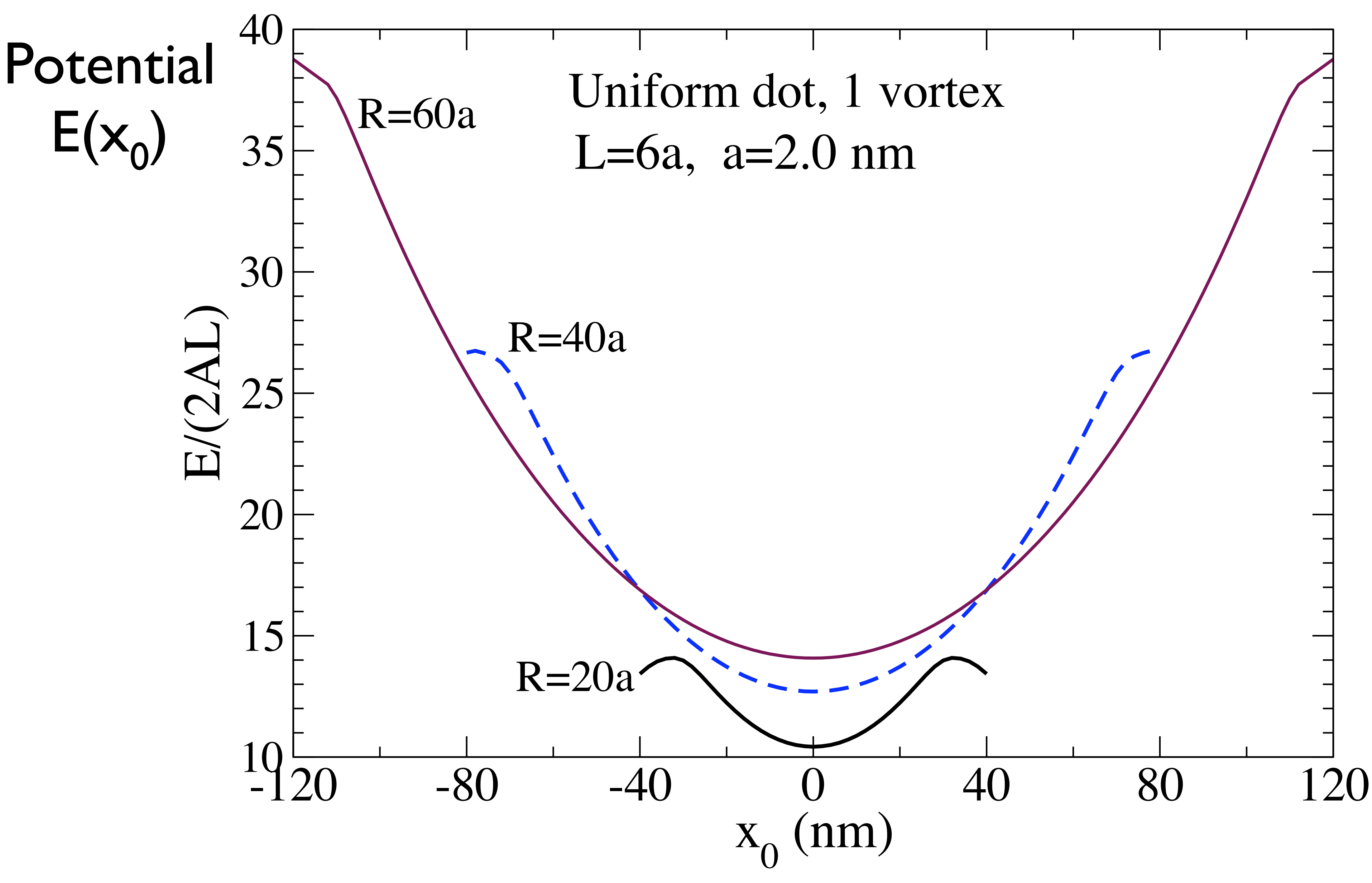

Example. Total energy of a vortex, $E(x_0) \approx \frac{1}{2} k_F x_0^2$

$a = 2.0$ nm, $\lambda_{ex} = 5.3$ nm, $\boxed{L = 4.0 \text{ nm},}$ $R = 40, 80, 120$ nm

Potential $E(x_0)$

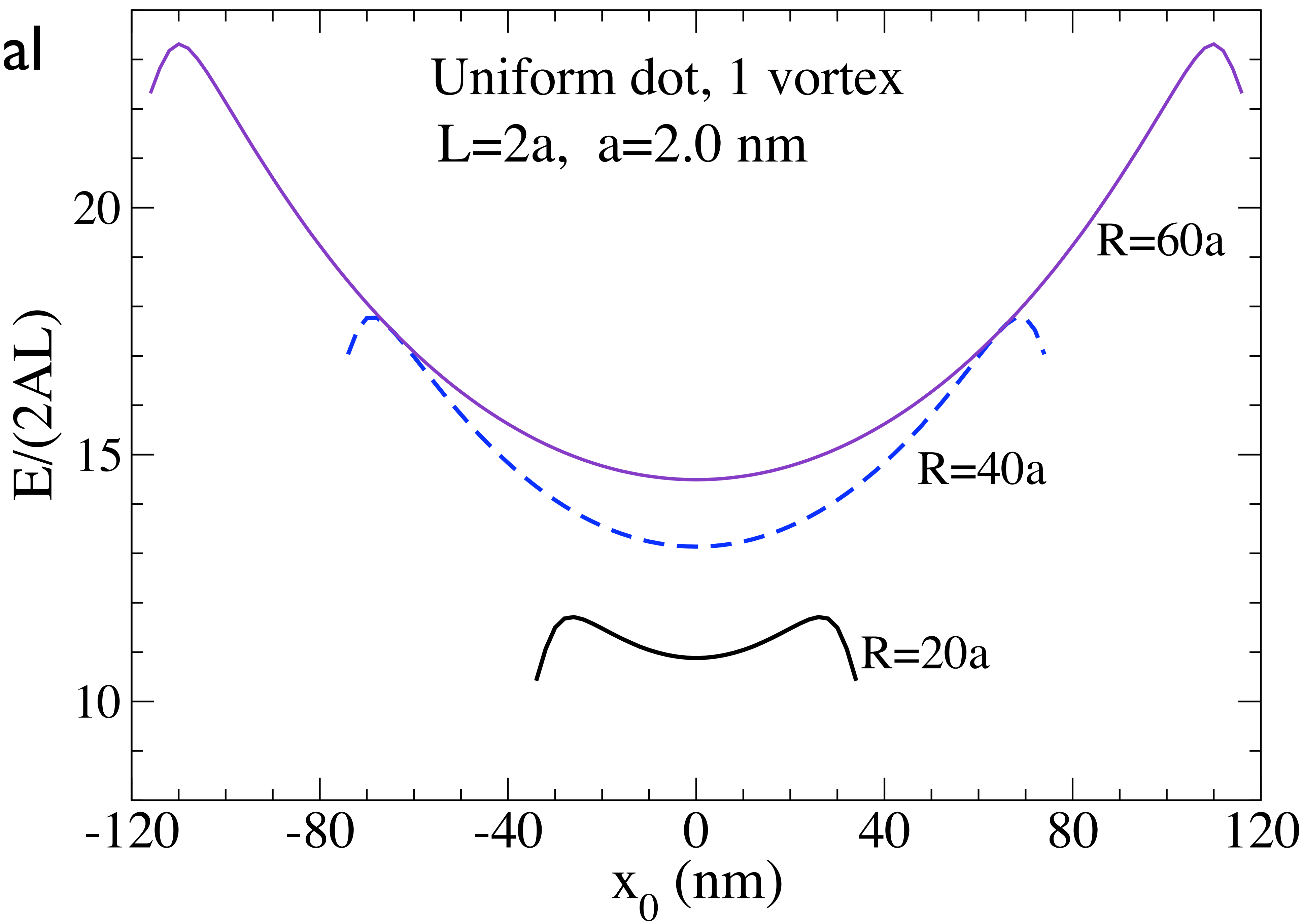

softer potentials

Gyrotropic movement

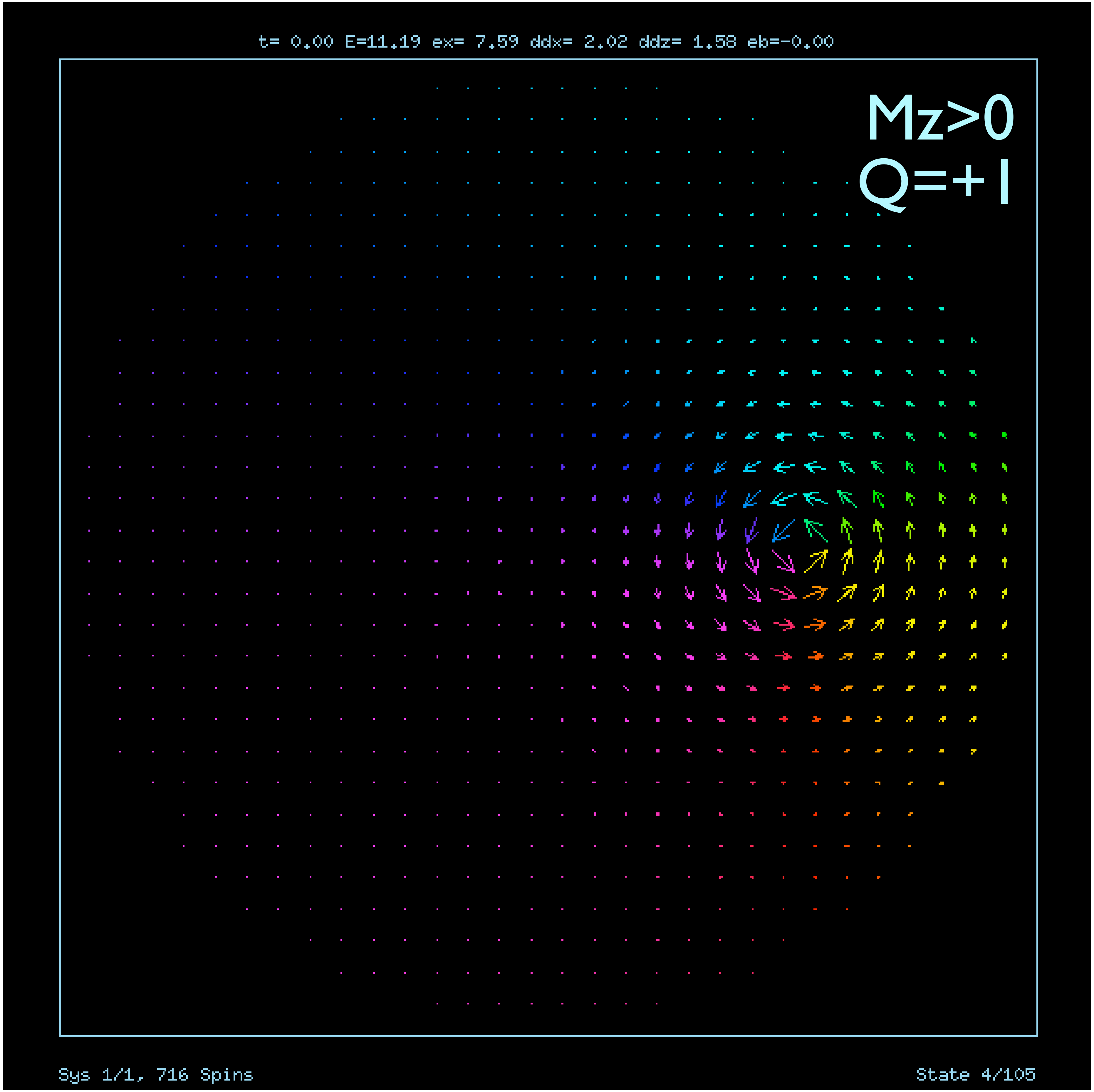

R=30 nm,
L=5 nm,
cells a=2.0 nm
α=0.02

gyrovector:

$$\mathbf{G} = 2\pi Q \hat{z}$$

$$Q = \pm 1$$

$$\boxed{\frac{\gamma}{m_0}\mathbf{F} + \mathbf{G} \times \mathbf{V} = 0.}$$

$$m_0 = \mu / a^2 = L M_s$$

With temperature T>0. For the movement in one cell:

$$\boxed{\frac{d\hat{m}}{d\tau} = \hat{m} \times \left(\vec{b} + \vec{b}_s\right) - \alpha \hat{m} \times \left[\hat{m} \times \left(\vec{b} + \vec{b}_s\right)\right]}$$

stochastic fields

fluctuation-dissipation theorem:

$$\langle b_s^\alpha(\tau)\, b_s^\beta(\tau')\rangle = 2\alpha\,\mathcal{T}\,\delta_{\alpha\beta}\,\delta(\tau - \tau') \qquad \mathcal{T} \equiv \frac{kT}{J_{\text{cell}}} = \frac{kT}{2AL}$$

(the stochastic fields carry thermal energy & power)

We can integrate with Heun's 2nd order algorithm:

A. Euler predictor step.
B. Trapezoid corrector step.

$$\int_{\tau_n}^{\tau_n + \Delta\tau} d\tau\ b_s^x(\tau) \longrightarrow \sigma_s w_n^x$$

ran( )

$$\sigma_s = \sqrt{2\alpha\mathcal{T}\,\Delta\tau}.$$

Spontaneous gyrotropic movement for T>0 (ellipse)

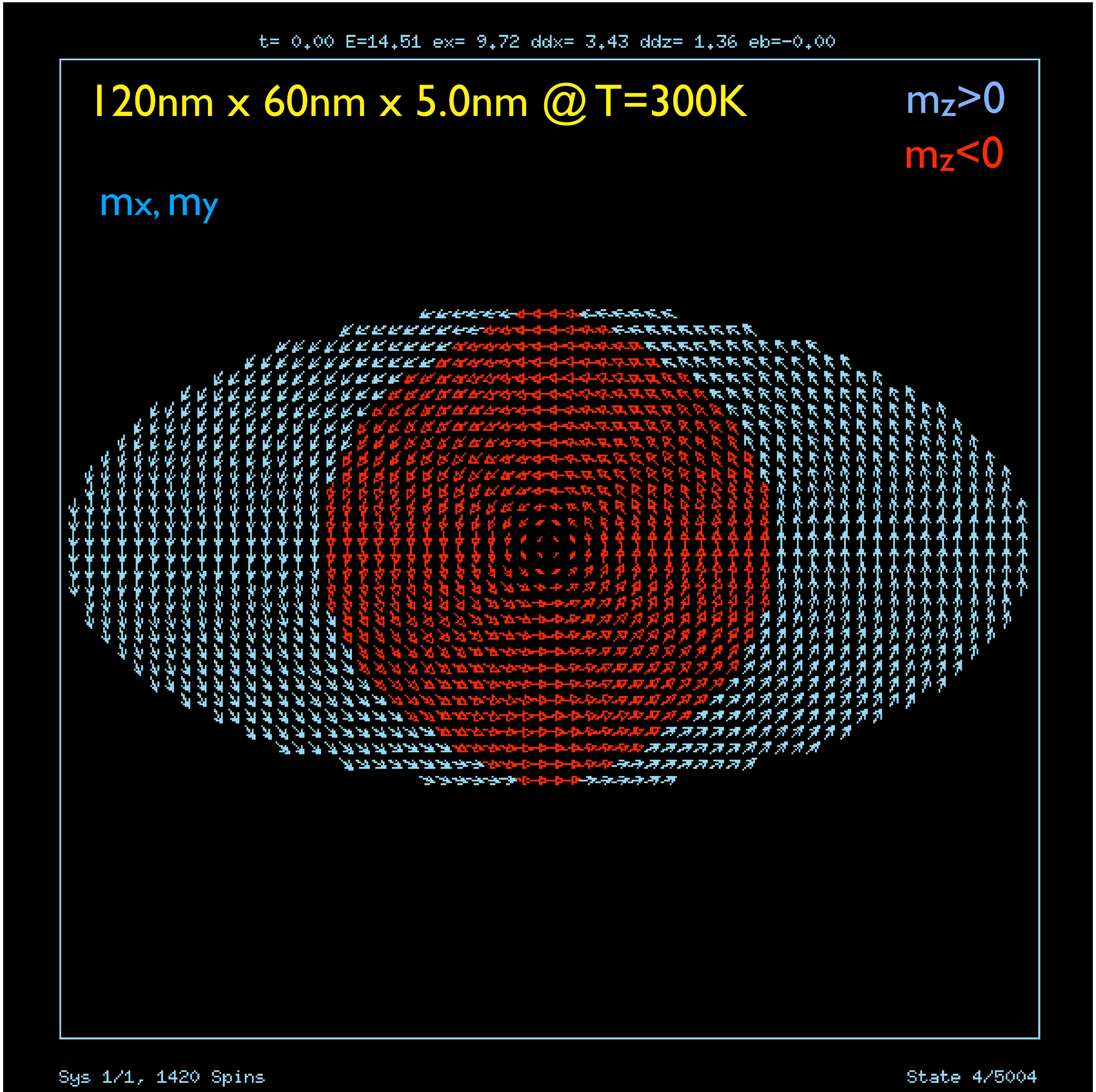

initial position
$x_0=y_0=0$

time unit
= 0.75 ps

Spontaneous gyrotropic movement for T>0 (ellipse)

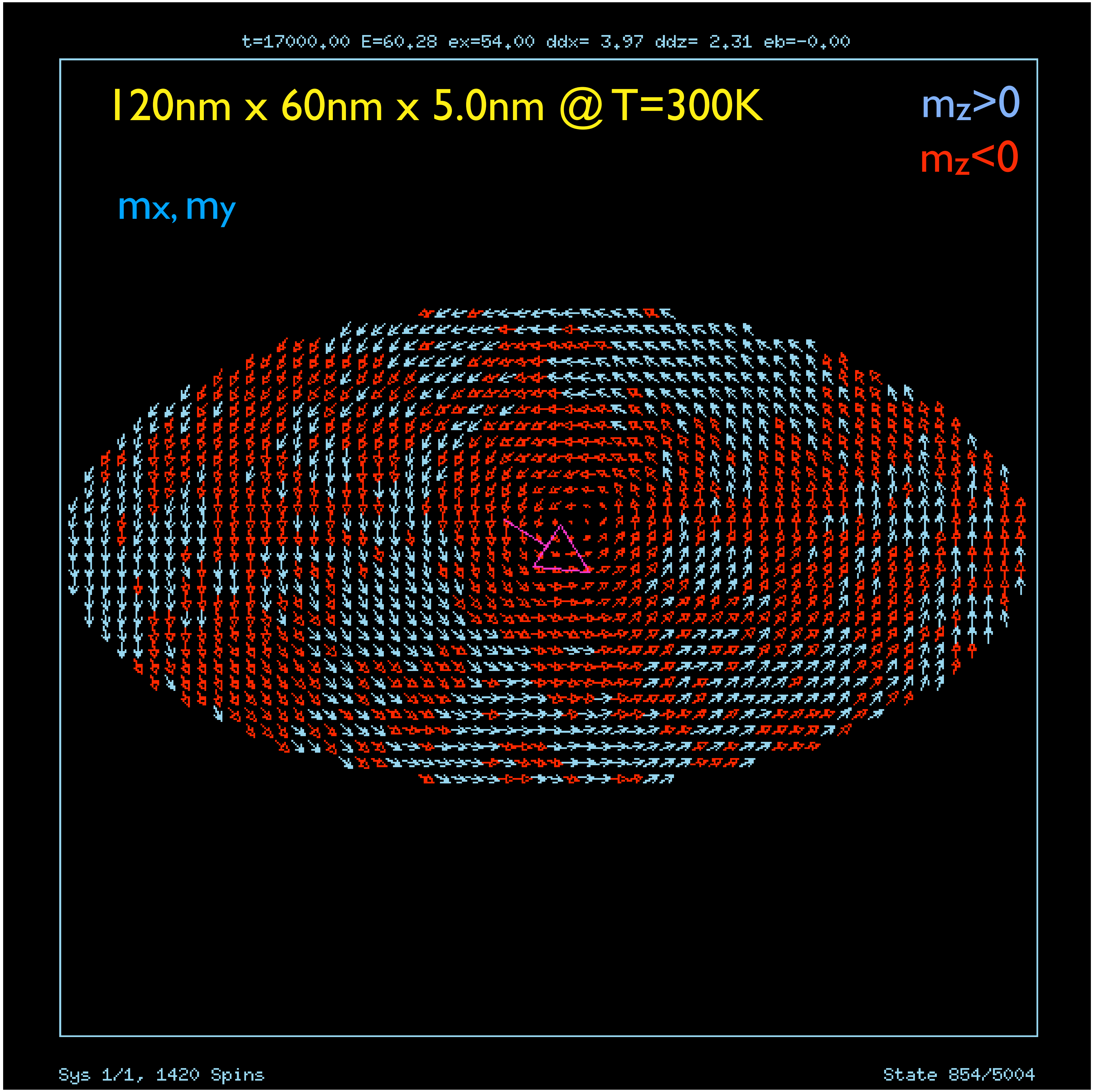

initial position
$x_0=y_0=0$

The large arrow
= <M>.
Note its faster
oscillations.

time unit
= 0.75 ps

The distribution of vortex radial coordinate in a circular nanodisk.
data points = simulation.   curves = Boltzman distribution.

$$p(r) = \beta k_F r\, e^{-\frac{1}{2}\beta k_F r^2}$$

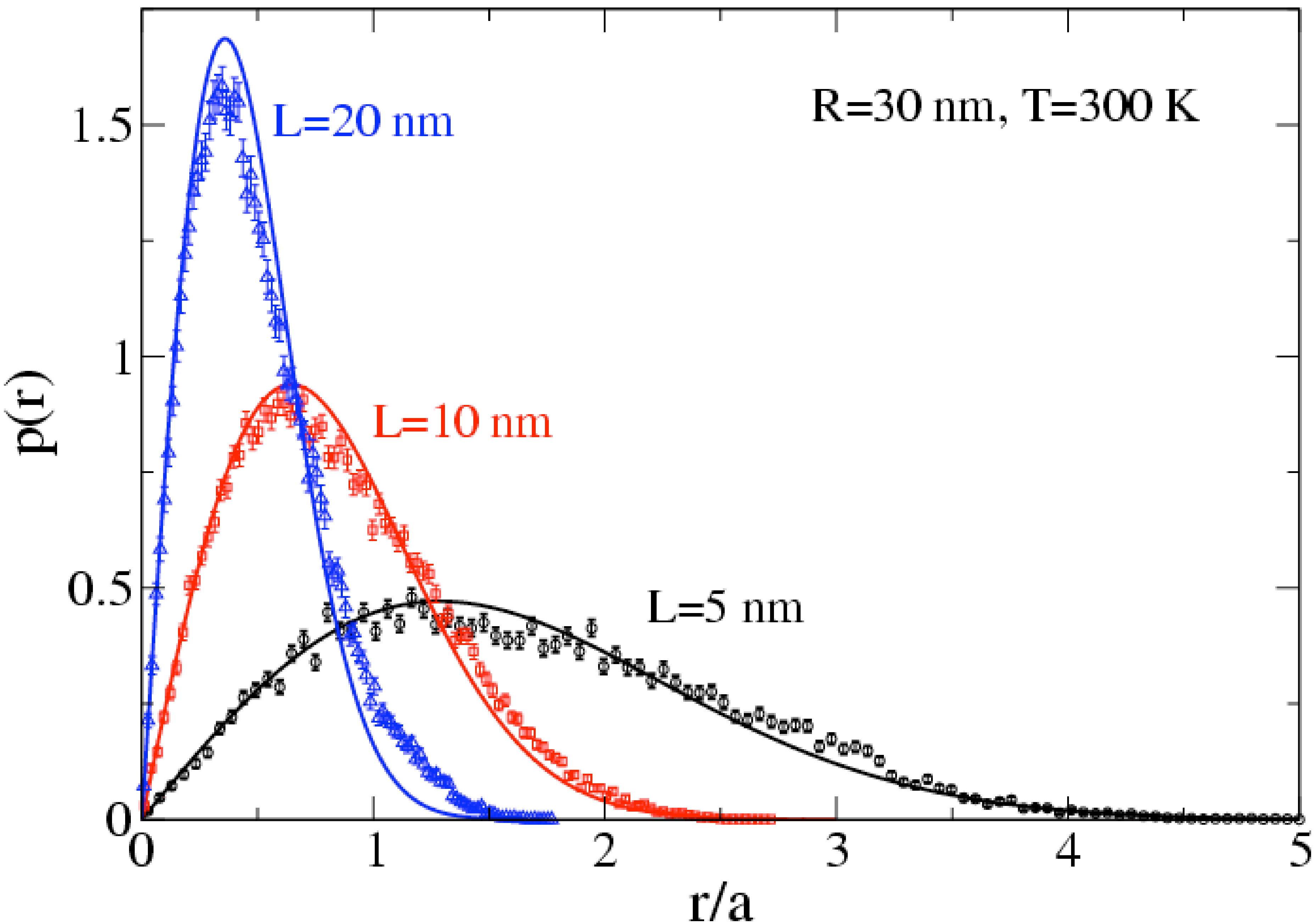

Wysin & Figueiredo

PHYSICAL REVIEW B 86, 104421 (2012)

2) Model for magnetic anisotropy of elliptical islands.

Total magnetic moment = μ. Single domain assumed.

$$\boxed{E = E_0 + K_1[1 - (\hat{\mu}\cdot\hat{x})^2] + K_3(\hat{\mu}\cdot\hat{z})^2}$$

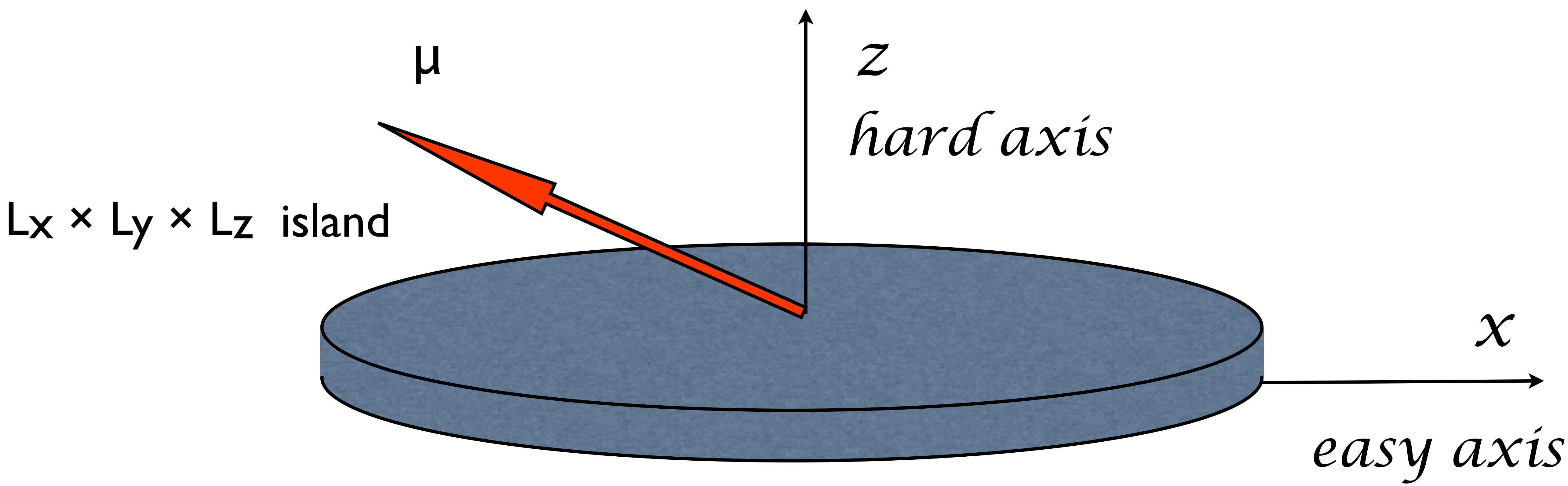

μ direction = (θ_m, ϕ_m)

angle from xy-plane

angle from x-axis

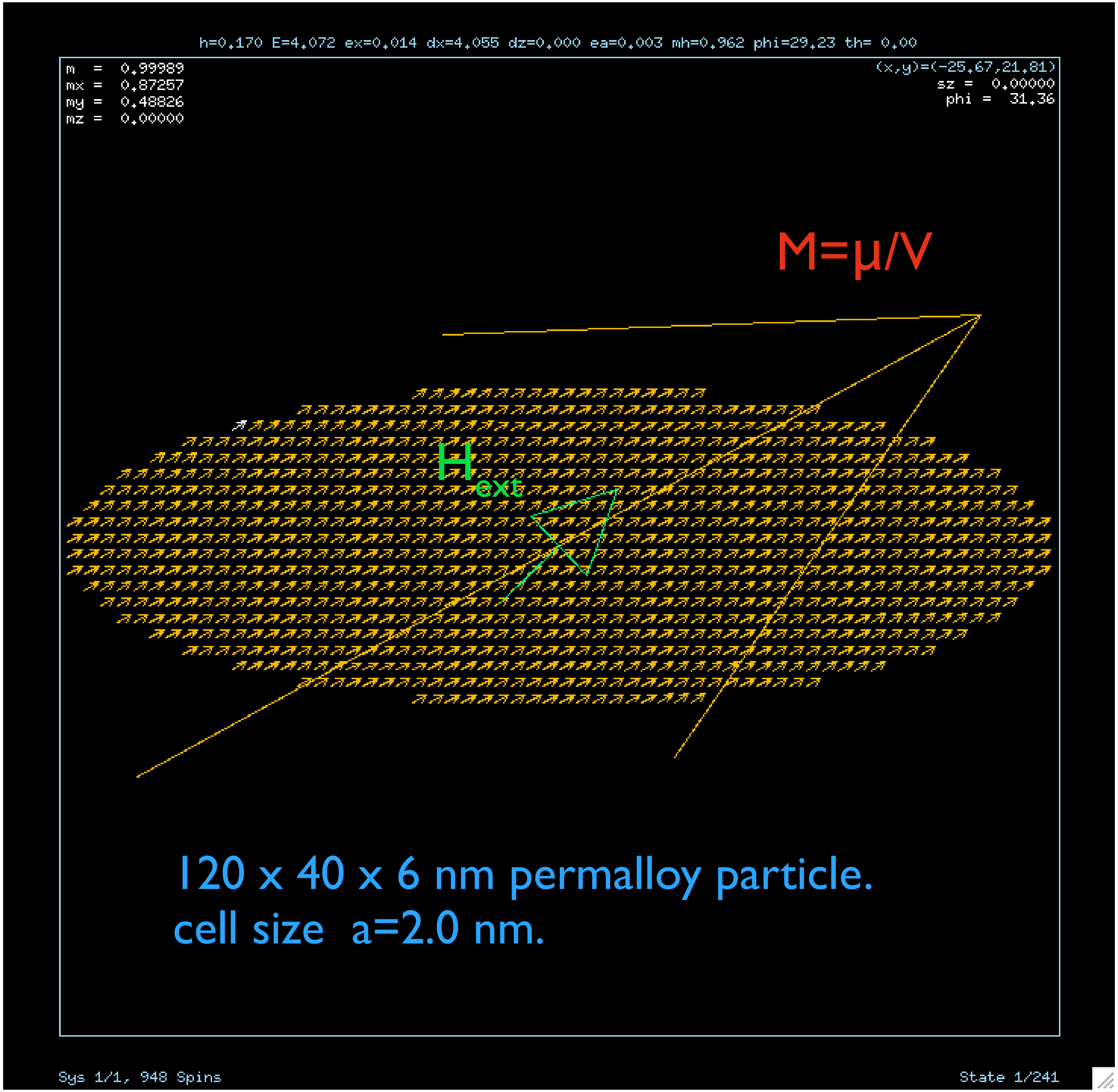
h=0.170 E=4.072 ex=0.014 dx=4.055 dz=0.000 ea=0.003 mh=0.962 phi=29.23 th= 0.00
m = 0.99989
mx = 0.87257
my = 0.48826
mz = 0.00000
(x,y)=(-25.67,21.81)
sz = 0.00000
phi = 31.36
M=μ/V
H ext
120 x 40 x 6 nm permalloy particle.
cell size a=2.0 nm.
Sys 1/1, 948 Spins
State 1/241

240 x 48 x 12 nm permalloy, reversal by an applied field at 10° to the axis.

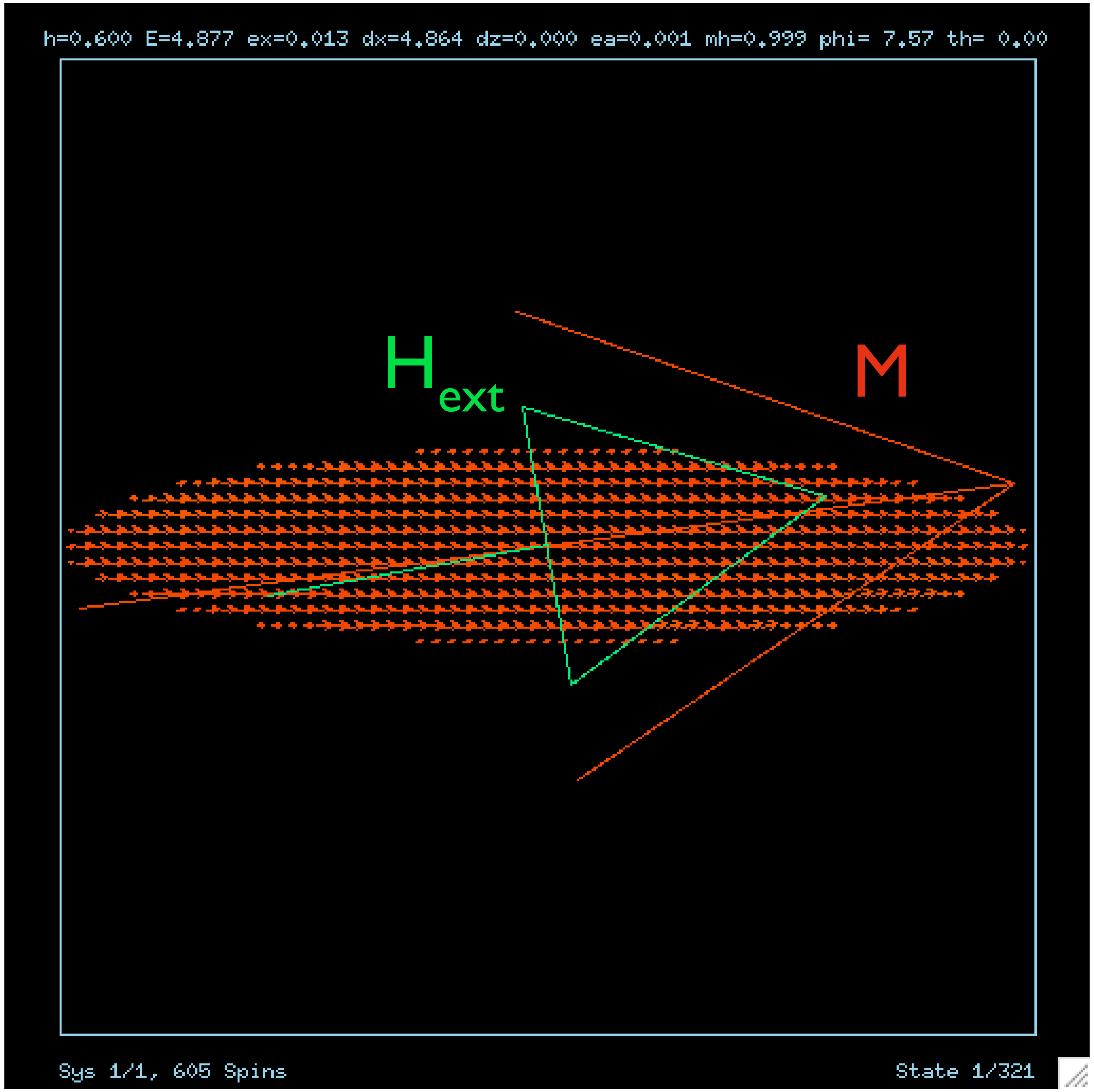

Obtained by energy minimization for each H_{ext}

M=μ/V

start here

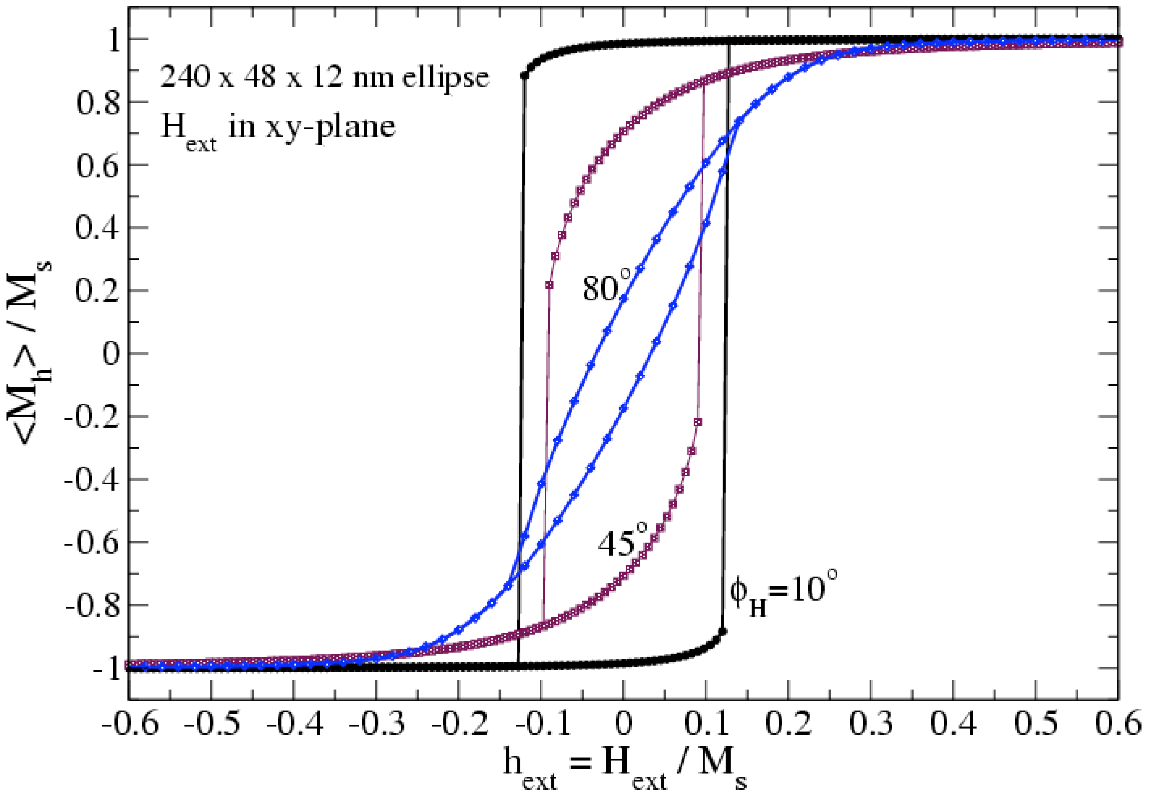

applied field

240 x 48 x 12 nm permalloy, reversal by an applied field at 10° to the axis.

Obtained by energy minimization for each H_{ext}

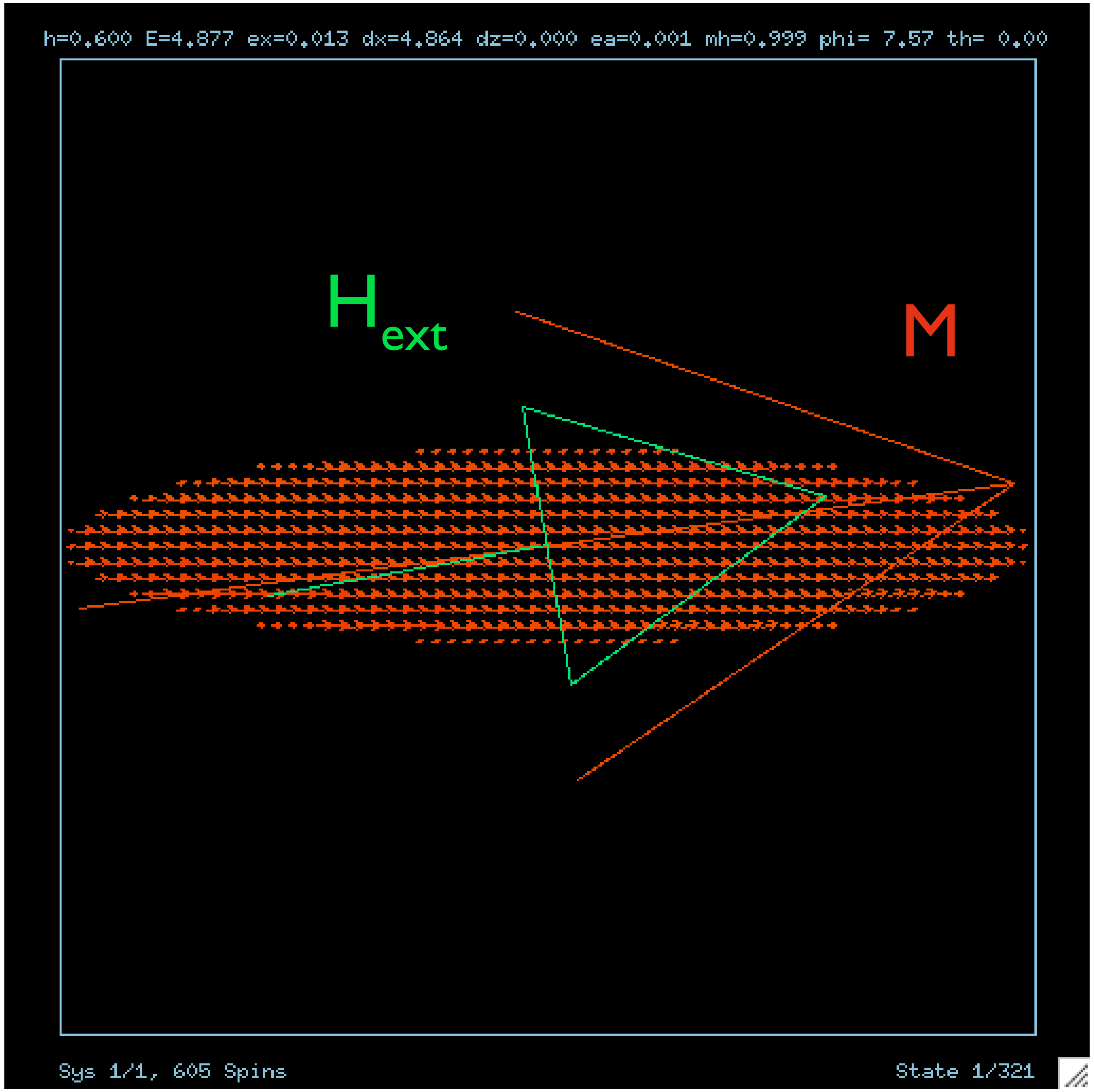

M=μ/V

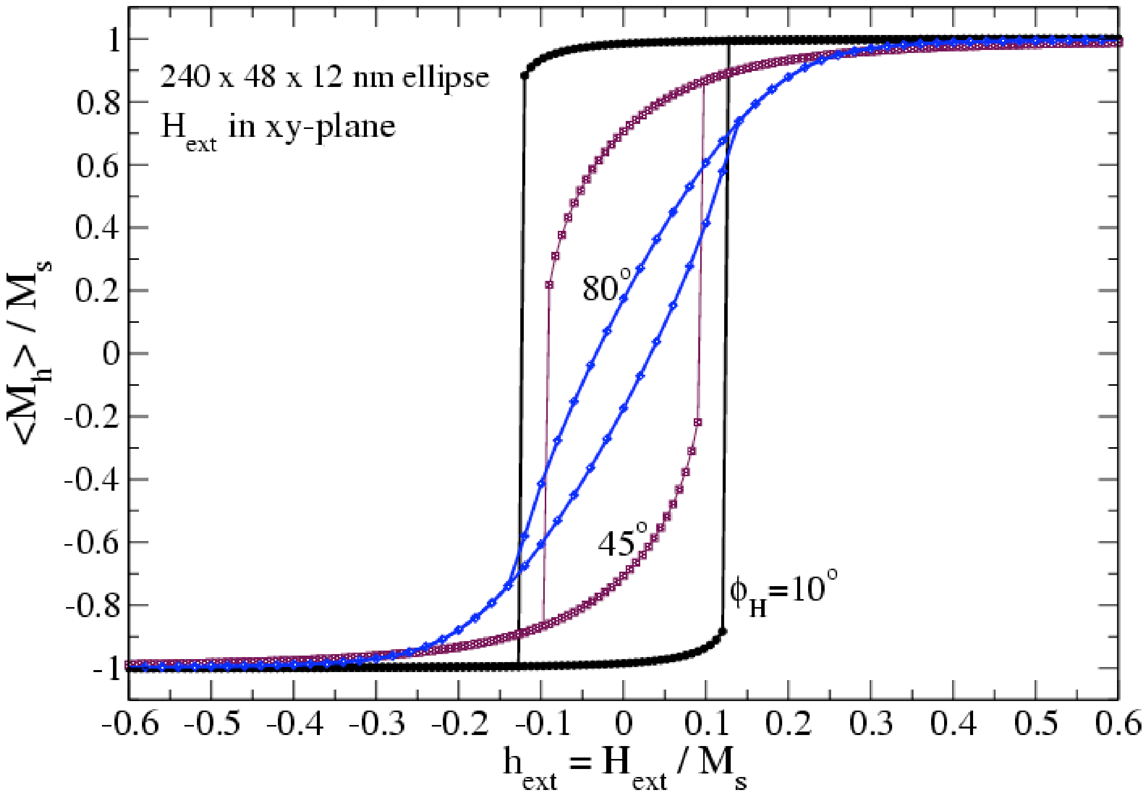

applied field

240 x 48 x 12 nm permalloy, reversal by an applied field at 45° to the axis.

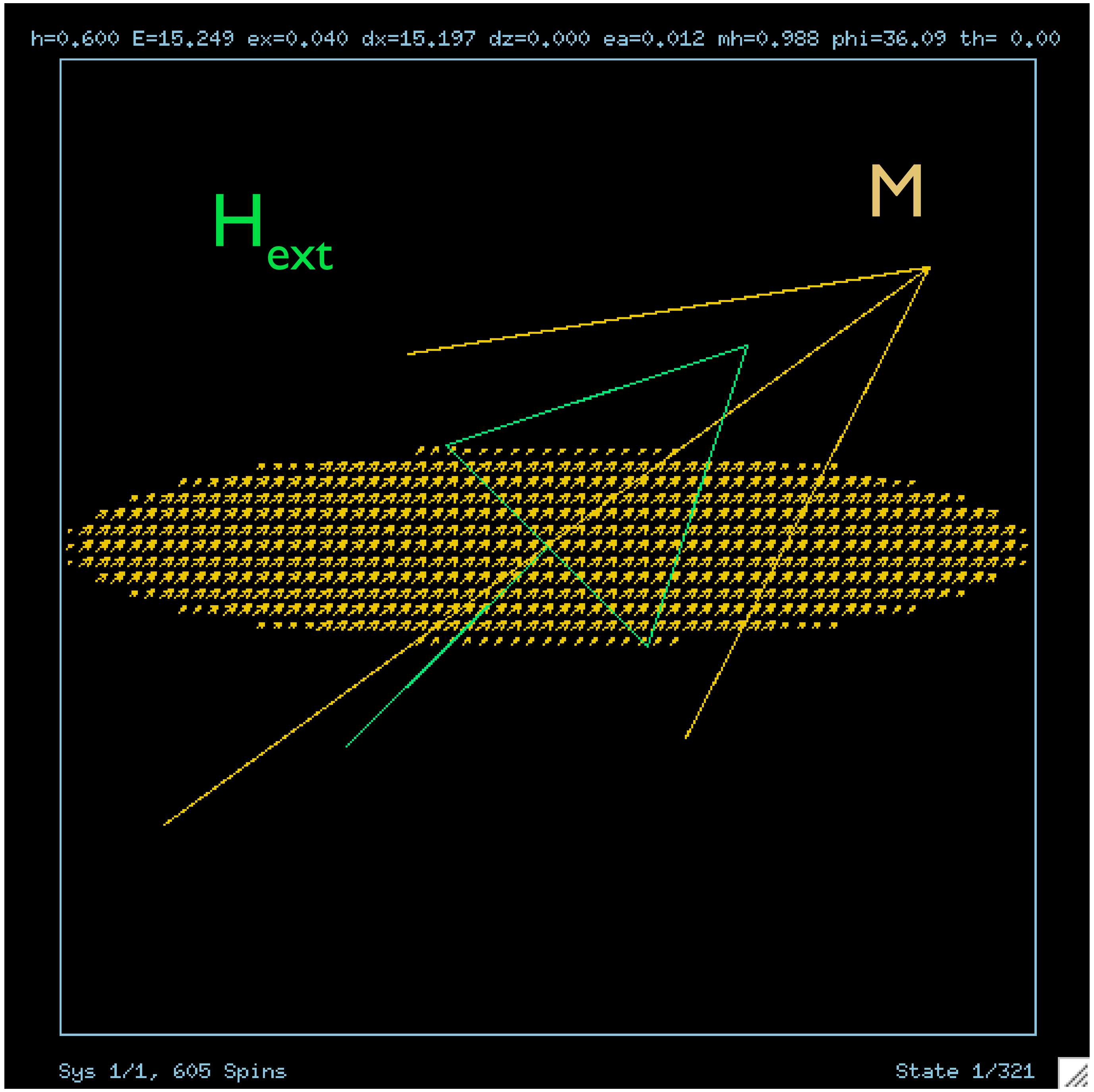

Obtained by energy minimization for each H_{ext}

$M=\mu/V$

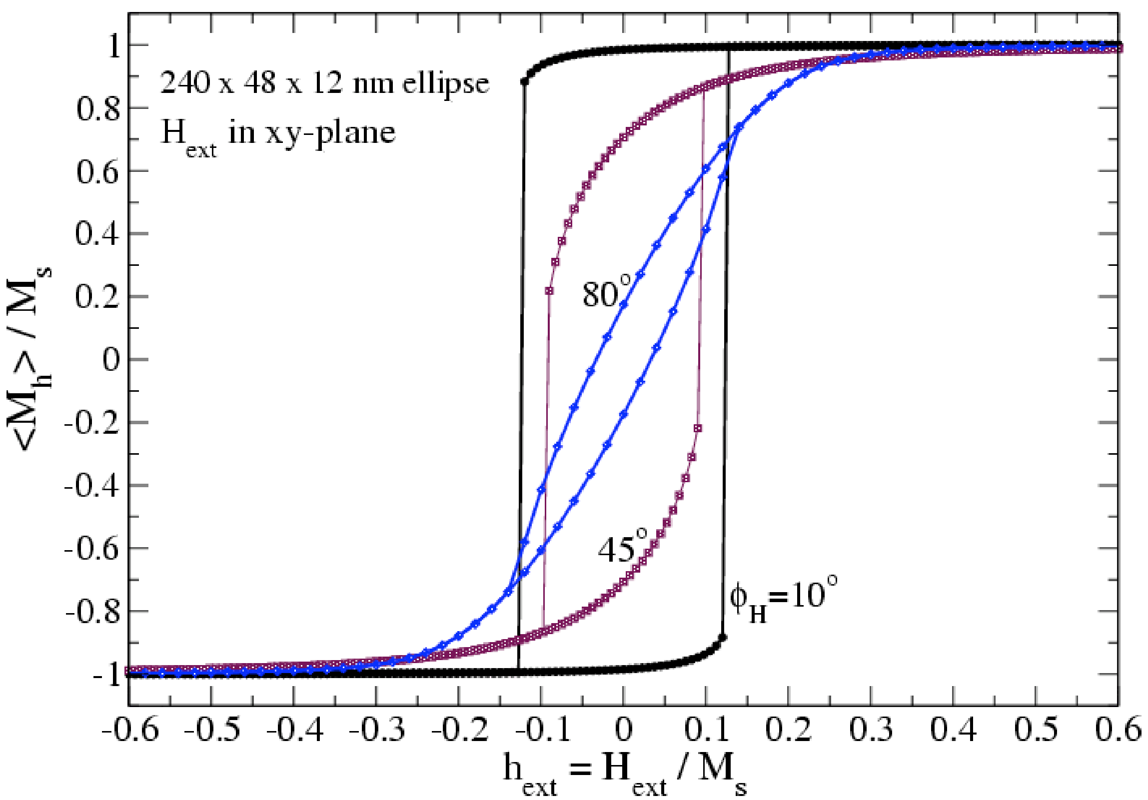

applied field

240 x 48 x 12 nm permalloy, reversal by an applied field at 80° to the axis.

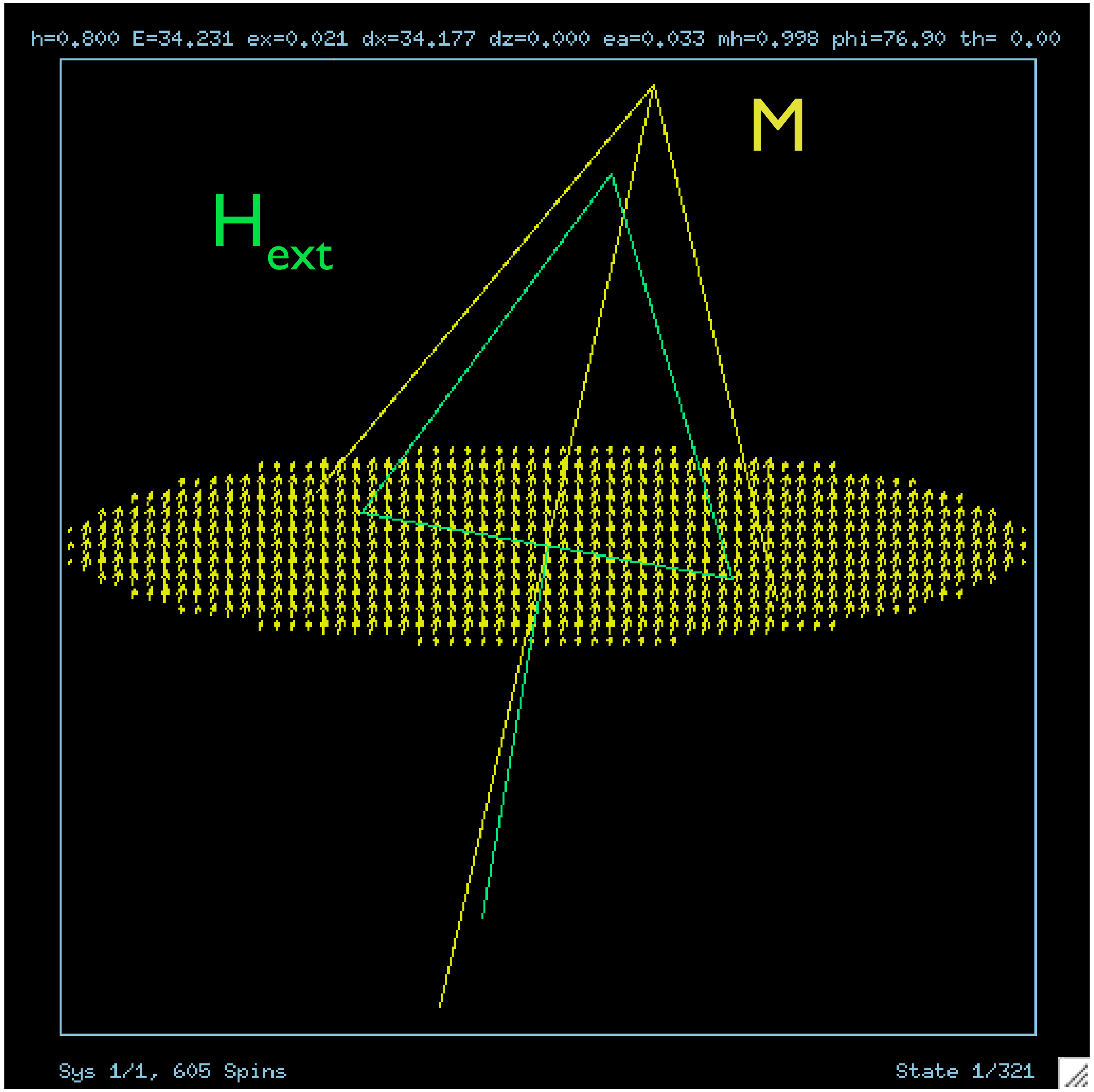

Obtained by energy minimization for each H_{ext}

$M=\mu/V$

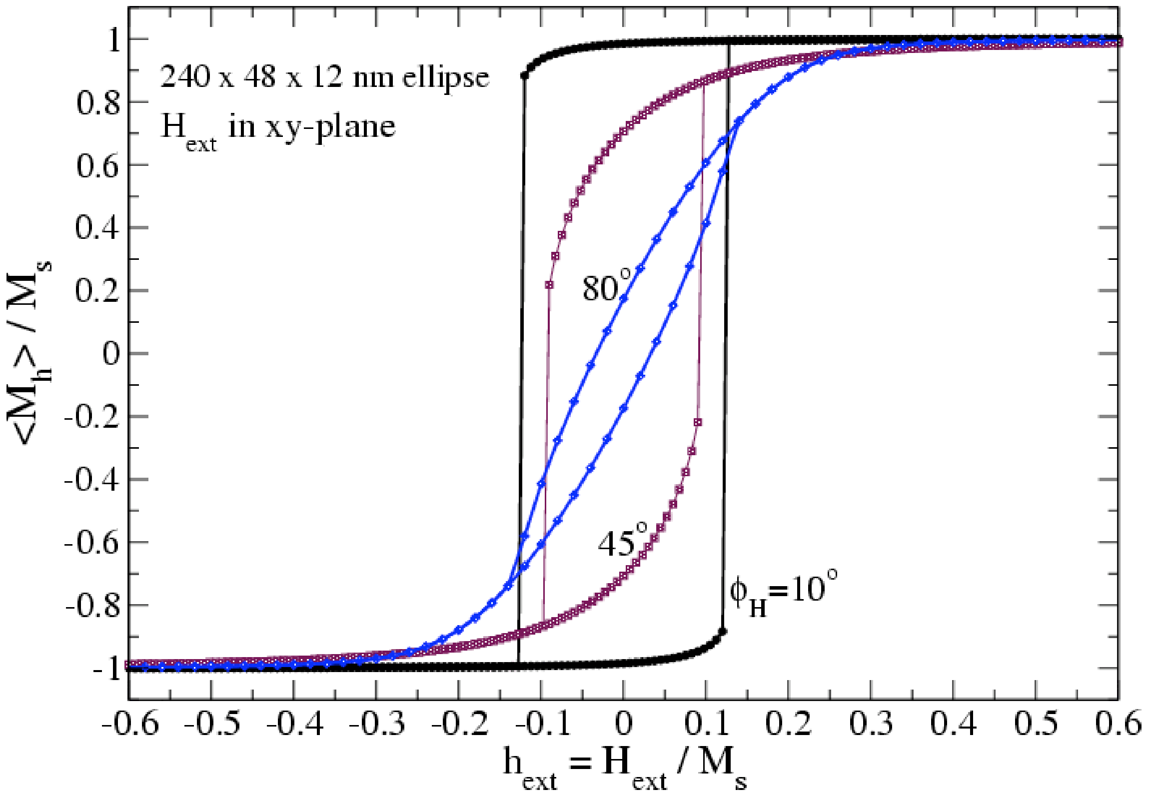

applied field

internal energy

$E_{int} = E_{ex} + E_{dd}$

$$E_{\rm int}(\phi_{\rm m}) = E_0 + K_1 \sin^2\phi_{\rm m}.$$

$K_1 = 31.5\ J_{\rm cell}$

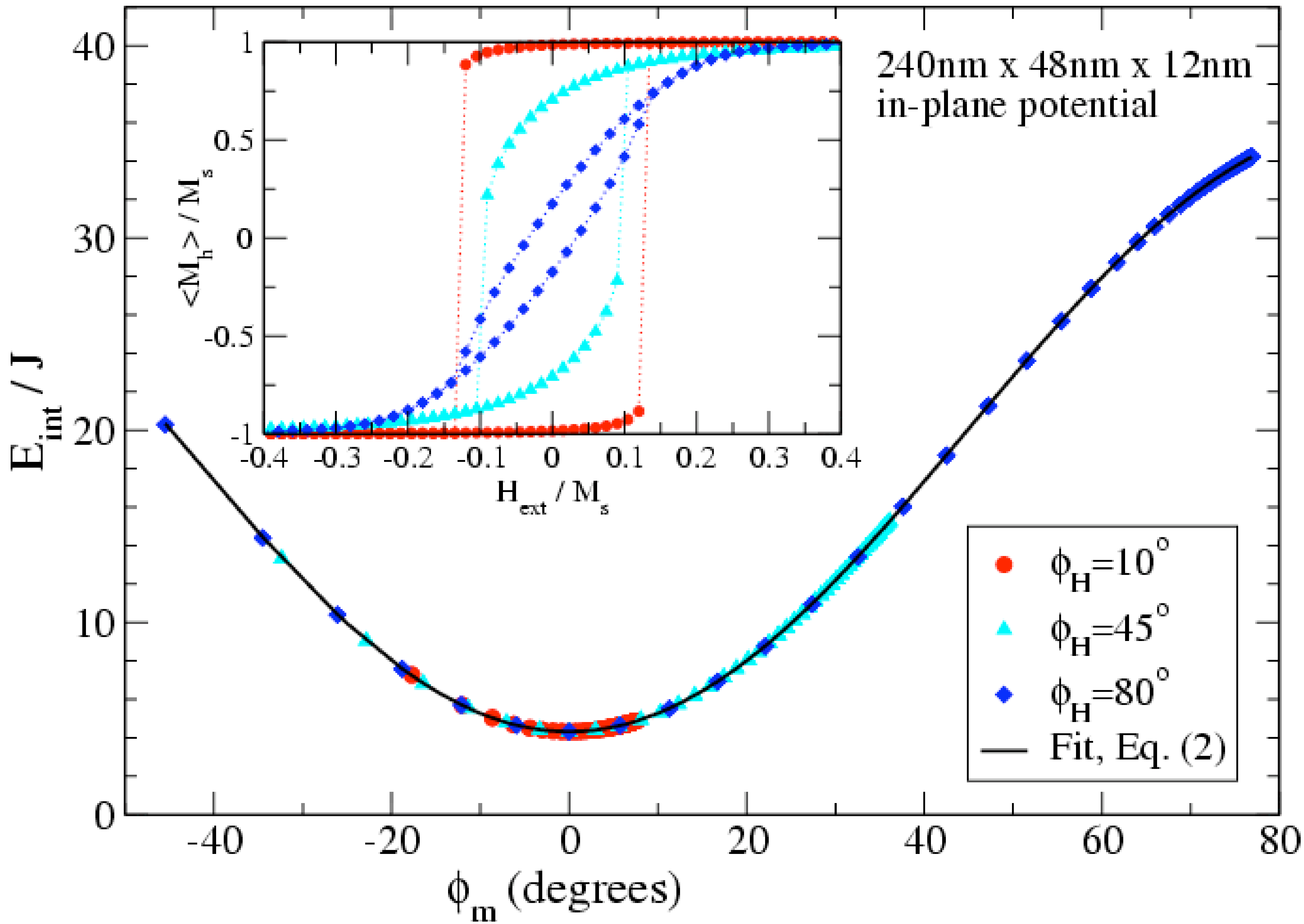

internal energy
$E_{int} = E_{ex} + E_{dd}$

$$E_{\mathrm{int}}(\theta_{\mathrm{m}}) = E_0 + (K_1 + K_3)\sin^2\theta_{\mathrm{m}}. \quad K_1+K_3=111\ J_{\mathrm{cell}}$$

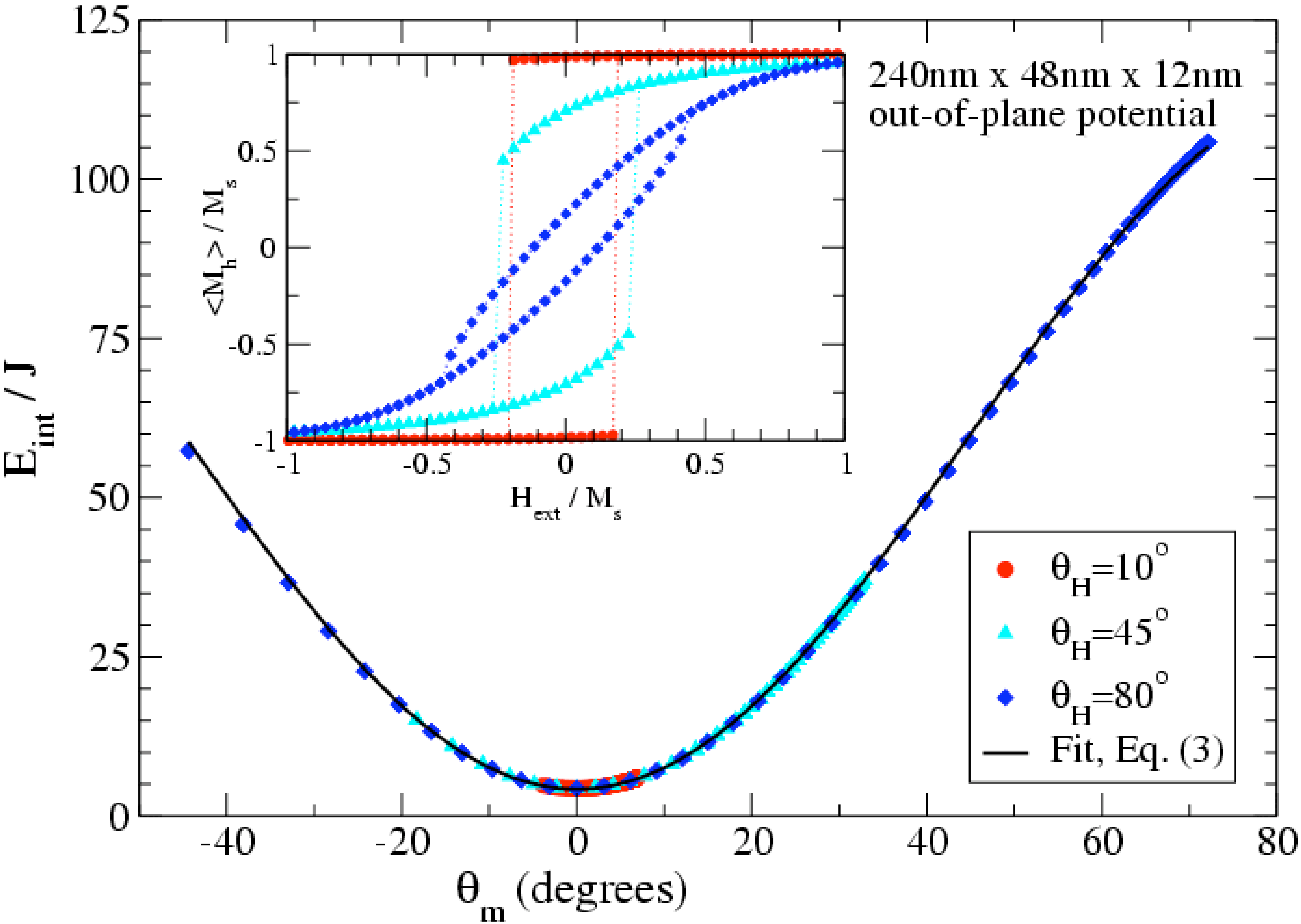

The results confirm the particle anisotropy for $L_x \times L_y \times L_z$ particles with high aspect ratios L_x/L_y:

$$\boxed{E = E_0 + K_1[1 - (\hat{\mu} \cdot \hat{x})^2] + K_3(\hat{\mu} \cdot \hat{z})^2}$$

J. Phys.: Condens. Matter **24** (2012) 296001

Table 1. Values of the in-plane anisotropy constant K_1 and out-of-plane anisotropy constant K_3 in units of $J = 2AL_z$ for different particle sizes and aspect ratios $g_1 = L_x/L_y$. All of the particles calculated have $g_3 = L_x/L_z = 20$.

	L_x					
	120 nm		240 nm		480 nm	
g_1	K_1	K_3	K_1	K_3	K_1	K_3
2	6.35J	72.7J	27.3J	287J	111J	1140J
3	7.32J	43.4J	31.9J	169J	134J	670J
5	6.96J	21.1J	31.5J	79.9J	133J	311J
8	7.39J	8.30J	29.5J	33.1J	118J	132J

Anisotropy constants per unit volume depend mainly on aspect ratios.

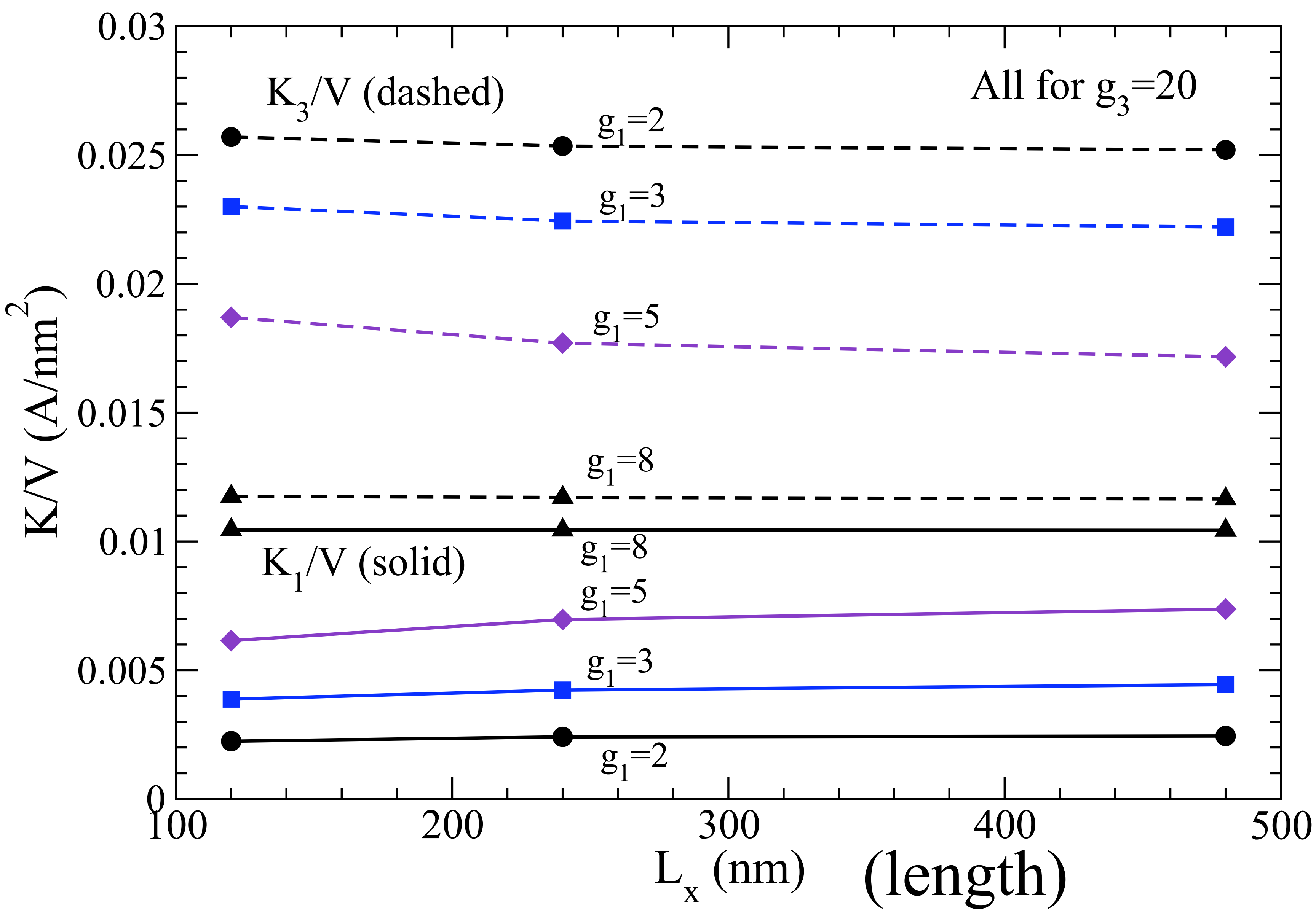

(length)

aspect ratios

$g_1 = L_x / L_y$

$g_3 = L_x / L_z$

Figure 3. The anisotropy constants K_1 (solid curves) and K_3 (dashed curves) scaled by elliptical particle volume, versus particle lengths, for the indicated g_1 aspect ratios. All data has $g_3 = 20$. The values of K/V are given in units of A nm^{-2}, where A is the exchange stiffness. K_1/V increases with aspect ratio while K_3/V decreases, and they become equal at high aspect ratio.

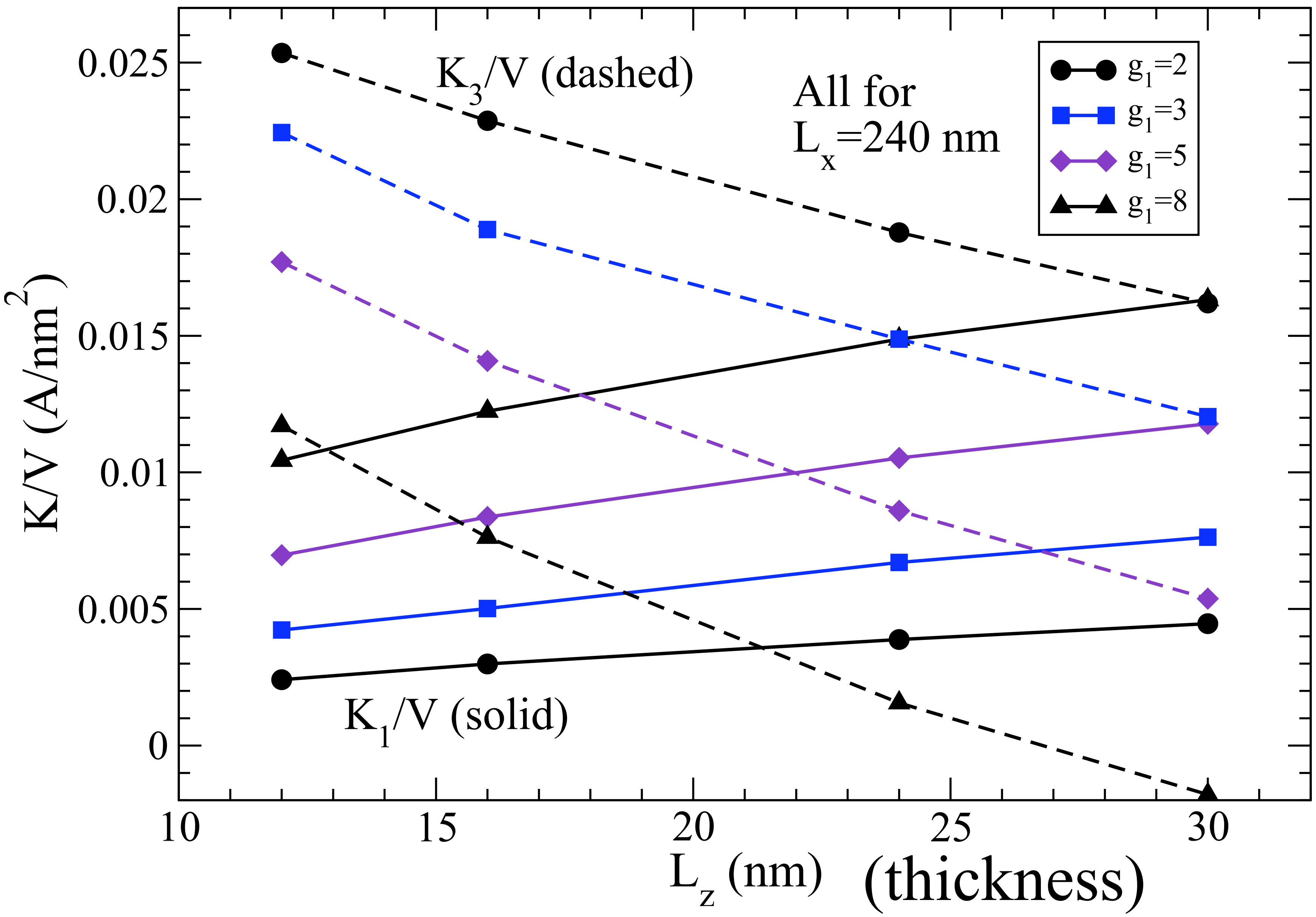

aspect ratios
$g_1=L_x/L_y$
$g_3=L_x/L_z$

Figure 6. The anisotropy constants K_1 (solid curves) and K_3 (dashed curves) scaled by elliptical particle volume, versus particle thicknesses, for the indicated g_1 aspect ratios. All the data is for particles of length $L_x = 240$ nm. The K_3/V constant crosses below zero for the thickest high aspect ratio particles, which have become needle-like and no longer satisfy the assumption of a thin particle. That is the case of a particle with only uniaxial anisotropy.

Dynamics and hysteresis in square lattice artificial spin ice

G M Wysin[1], W A Moura-Melo[2], L A S Mól[2,3,4] and A R Pereira[2]

New Journal of Physics **15** (2013) 045029 (24pp)

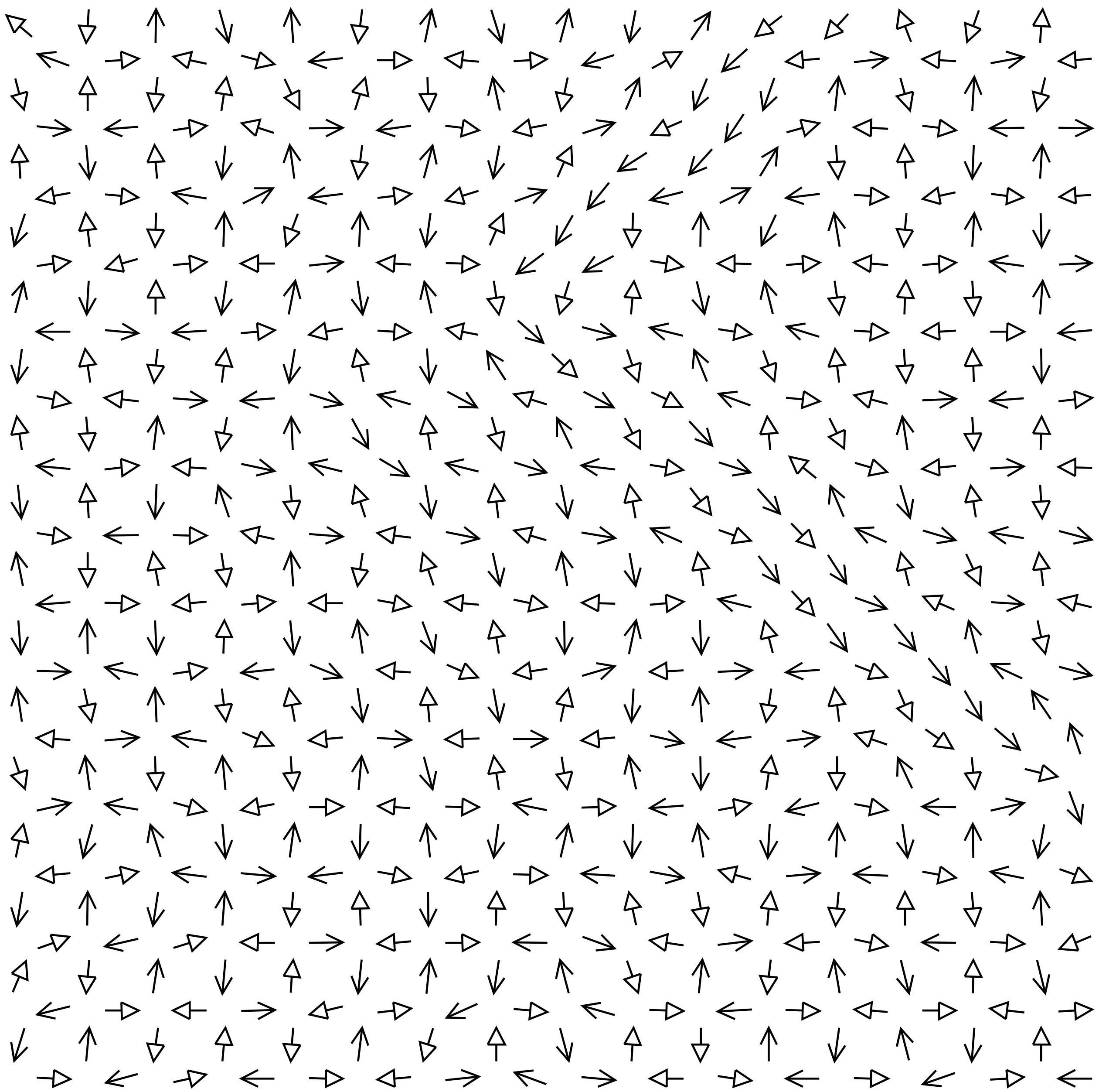

Figure 1. A 16 × 16 model system with $d = k_1 = k_3 = 0.1$, in a metastable state at temperature $k_B T/\varepsilon = 0.025$, from a hysteresis scan (this is a state at $h_{ext} = 0$). Most of the system is locally close to the $Z = +1$ ground state. The upper right-hand corner is locally near the $Z = -1$ ground state, and there is a bent domain wall connecting the two regions. For interior charge sites (junction points of four islands), there happens to be no discrete monopole charge present: all $q_k = 0$ and the discrete $\rho_m = 0$.

3) Artificial spin-ice. Arrays of elongated magnetic islands, dominated by anisotropy & dipole-dipole interactions.

Each arrow = one island.

Island rows are alternately aligned along x or y-axes in this artifical square ice.

This system has two degenerate ground states.

Mimics the behavior of 3D spin ices of rare earths in lattice of corner sharing tetrahedra of a pyrochlore structure.

Interactions = dipolar + shape anisotropy + external field

$$\mathcal{H} = -\frac{\mu_0}{4\pi}\frac{\mu^2}{a^3}\sum_{i>j}\frac{[3(\hat{\mu}_i\cdot\hat{r}_{ij})(\hat{\mu}_j\cdot\hat{r}_{ij})-\hat{\mu}_i\cdot\hat{\mu}_j]}{(r_{ij}/a)^3}+\sum_i\{\underbrace{K_1[1-(\hat{\mu}_i\cdot\hat{u}_i)^2]}_{\text{easy axis}}+\underbrace{K_3(\hat{\mu}_i\cdot\hat{z})^2}_{\text{hard axis}}-\vec{\mu}_i\cdot\vec{B}_{\text{ext}}\}$$

dipolar energy scale = D

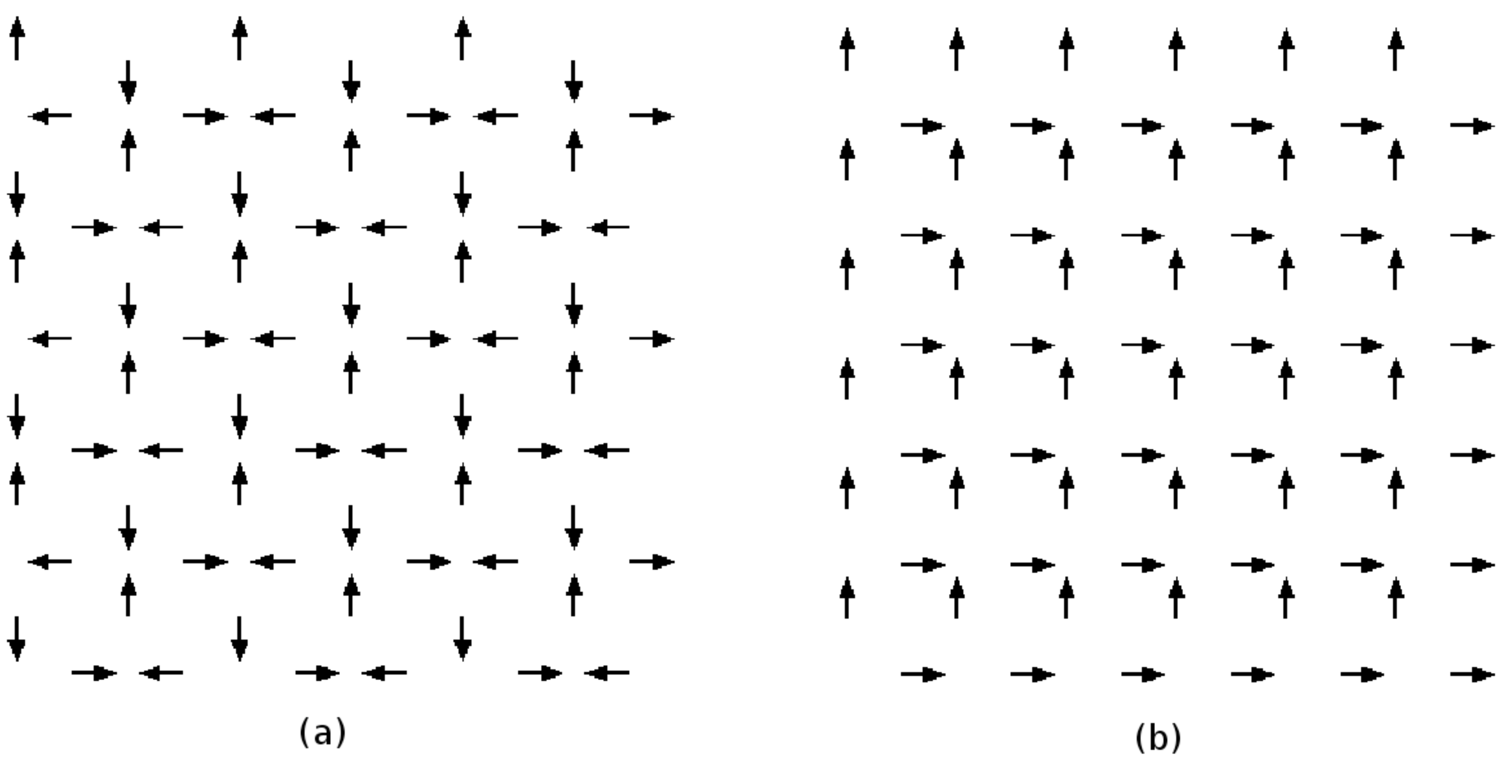

Ice-rule:

For lowest energy, equal numbers of inward and outward pointing dipoles at each vertex.

FIG. 2: (a) Configuration of the ground-state obtained for $L = 6a$, in exact agreement with that experimentally observed. Note that the ice rules are manifested at each vertex. This is the case in which the topology demands the minimum energy (see Fig. (3)). (b) Another configuration also respecting the ice rule, but displaying a topology which costs more energy. (Mol et al 2008.)

deviations from the ice rule

⇒ higher energy and monopole "charges"

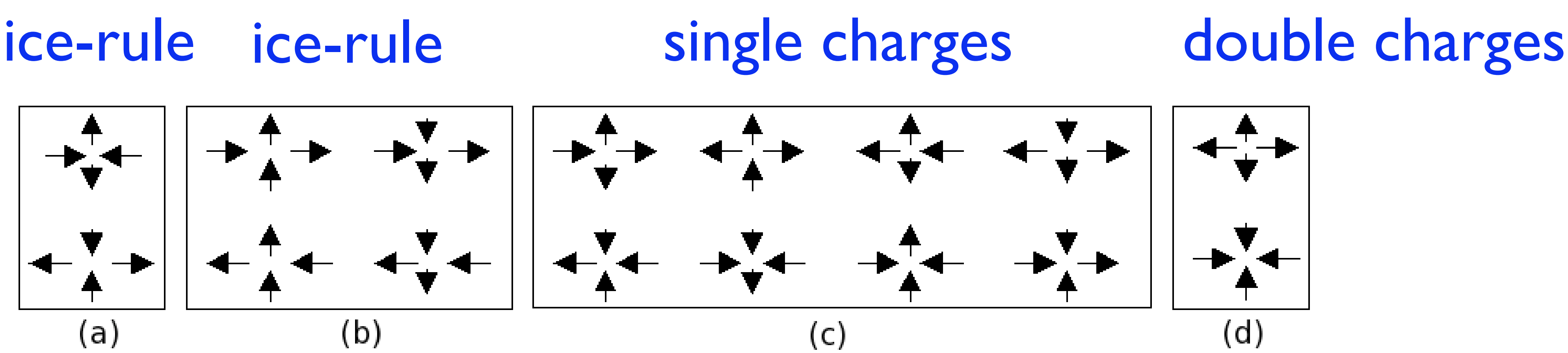

FIG. 3: The 4 distinct topologies and the 16 possible magnetic moment configurations on a vertex of 4 islands. Although configurations (a) and (b) obey the ice rule, the topology of (a) is more energetically favorable than that of (b). Hamiltonian (1) correctly yields to the true ground-state based on topology (a), without further assumptions. Topologies (c) and (d) does not obey the ice rule. Particularly, (c) implies in a monopole with charge Q_M.

How do the excitations behave as particles, interact with each other, and contribute to thermodynamics?

artificial ice model

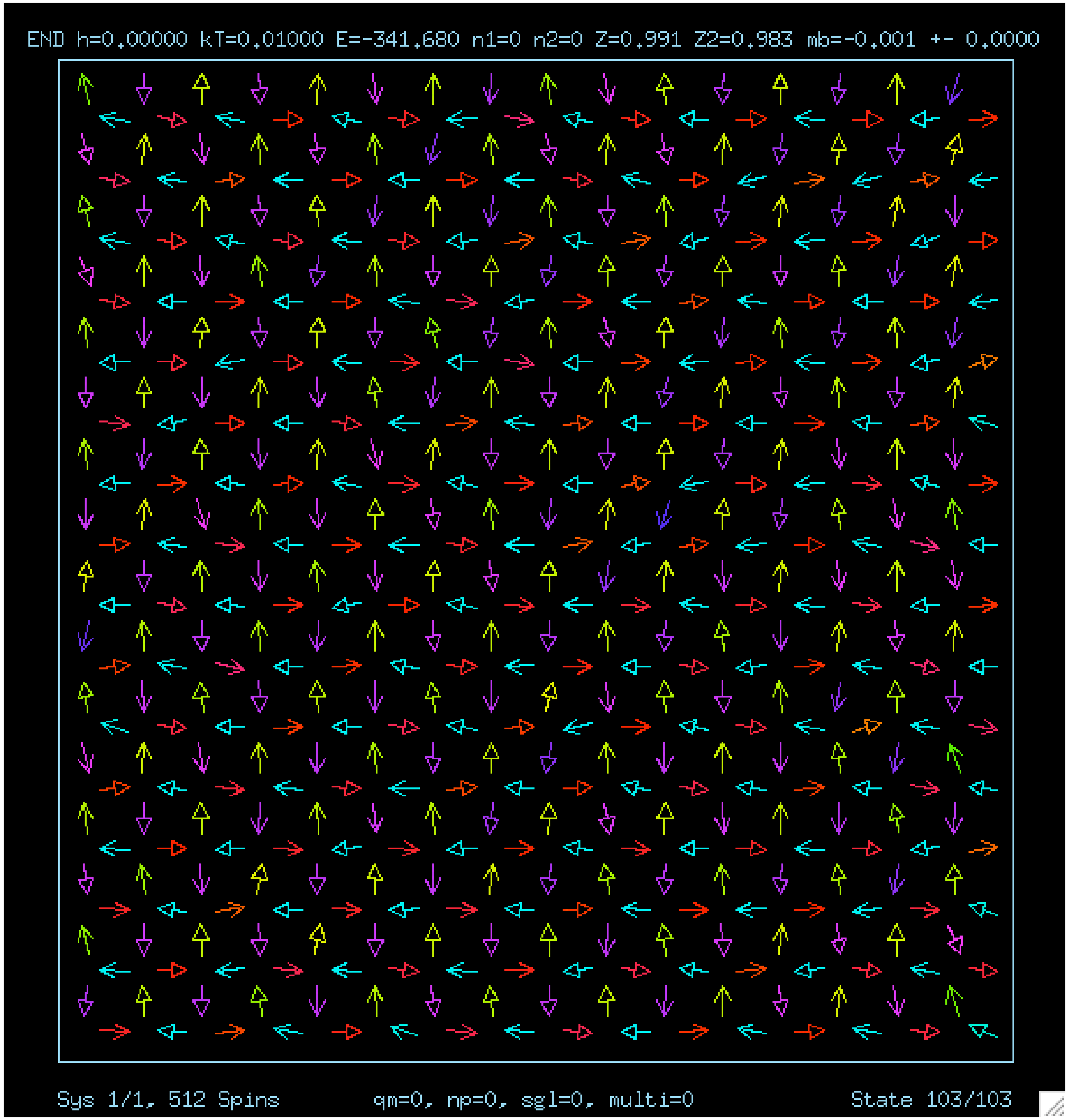

$D = 0.1$

$K_1 = 0.1$

$K_3 = 0.5$

$kT = 0.01$

$\approx$ ground state

(from long-time Langevin dynamics)

$$D = \frac{\mu_0}{4\pi}\frac{\mu^2}{a^3}$$

artificial ice model

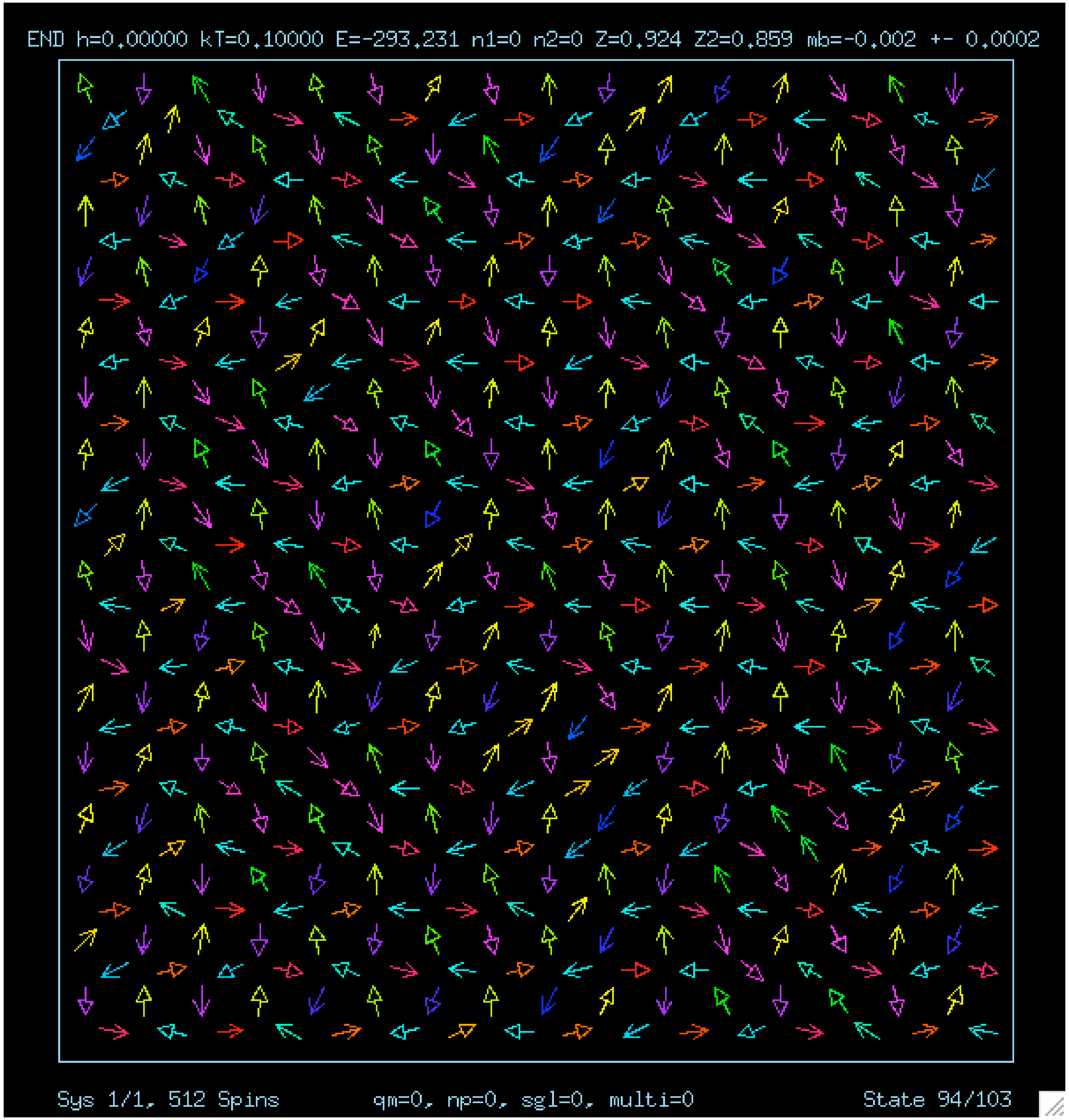

$D = 0.1$
$K_1 = 0.1$
$K_3 = 0.5$

$kT = 0.10$

> ground state

(from long-time Langevin dynamics)

artificial ice model

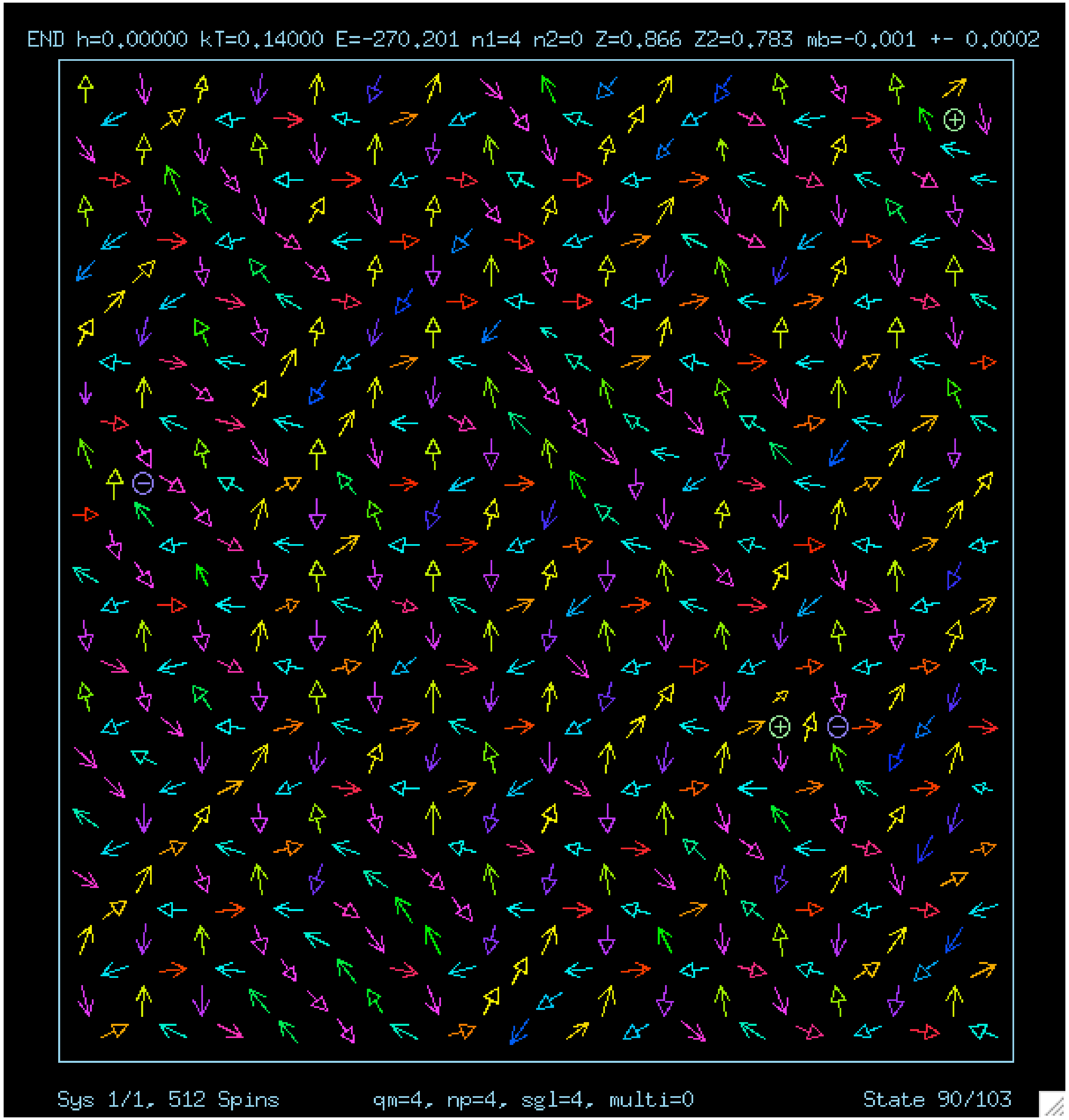

$D = 0.1$

$K_1=0.1$

$K_3=0.5$

$kT=0.14$

few monopoles

(from long-time Langevin dynamics)

artificial ice model

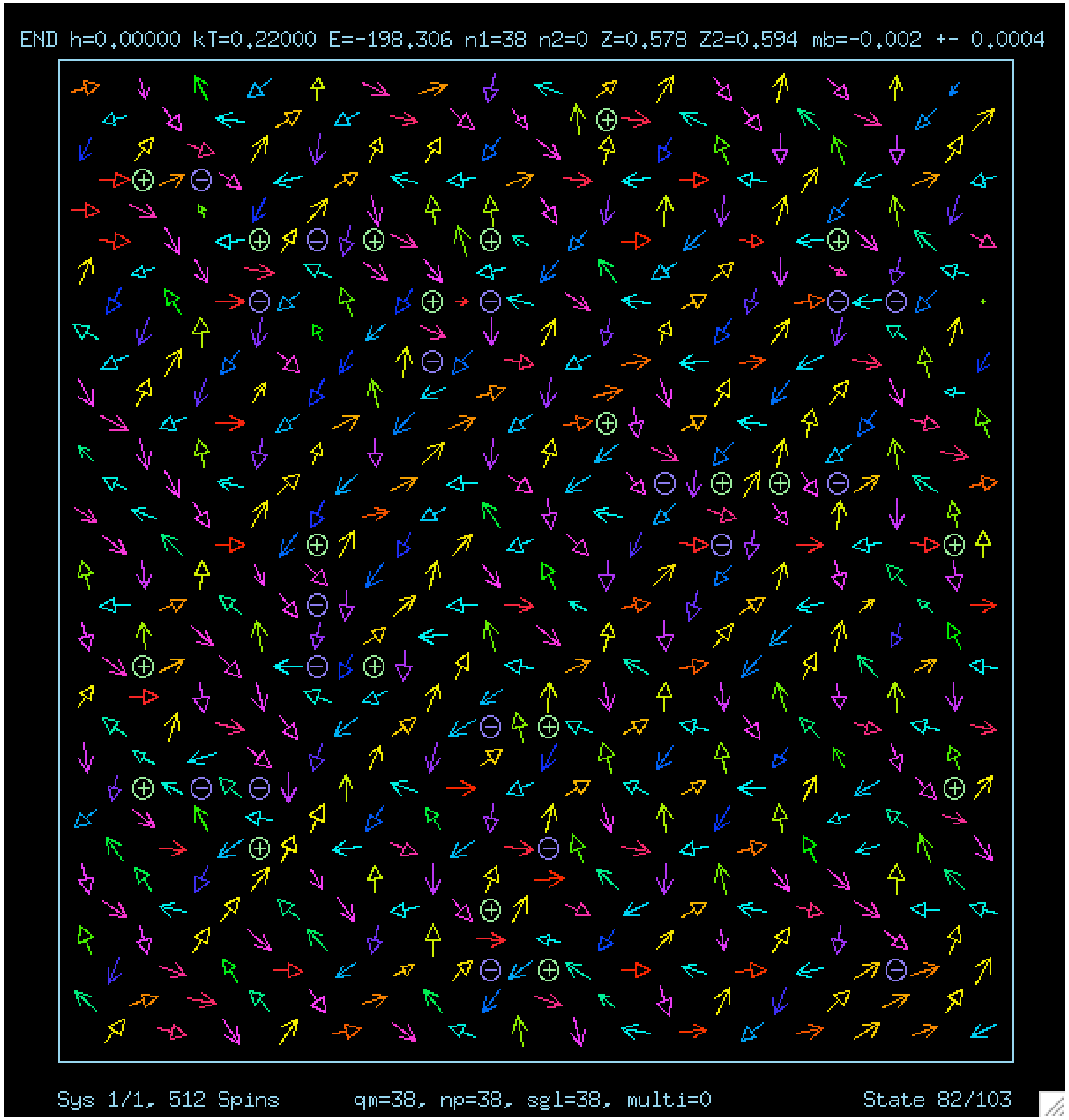

$D = 0.1$

$K_1=0.1$

$K_3=0.5$

$kT=0.22$

≈ transition to high-T phase

(from long-time Langevin dynamics)

artificial ice model

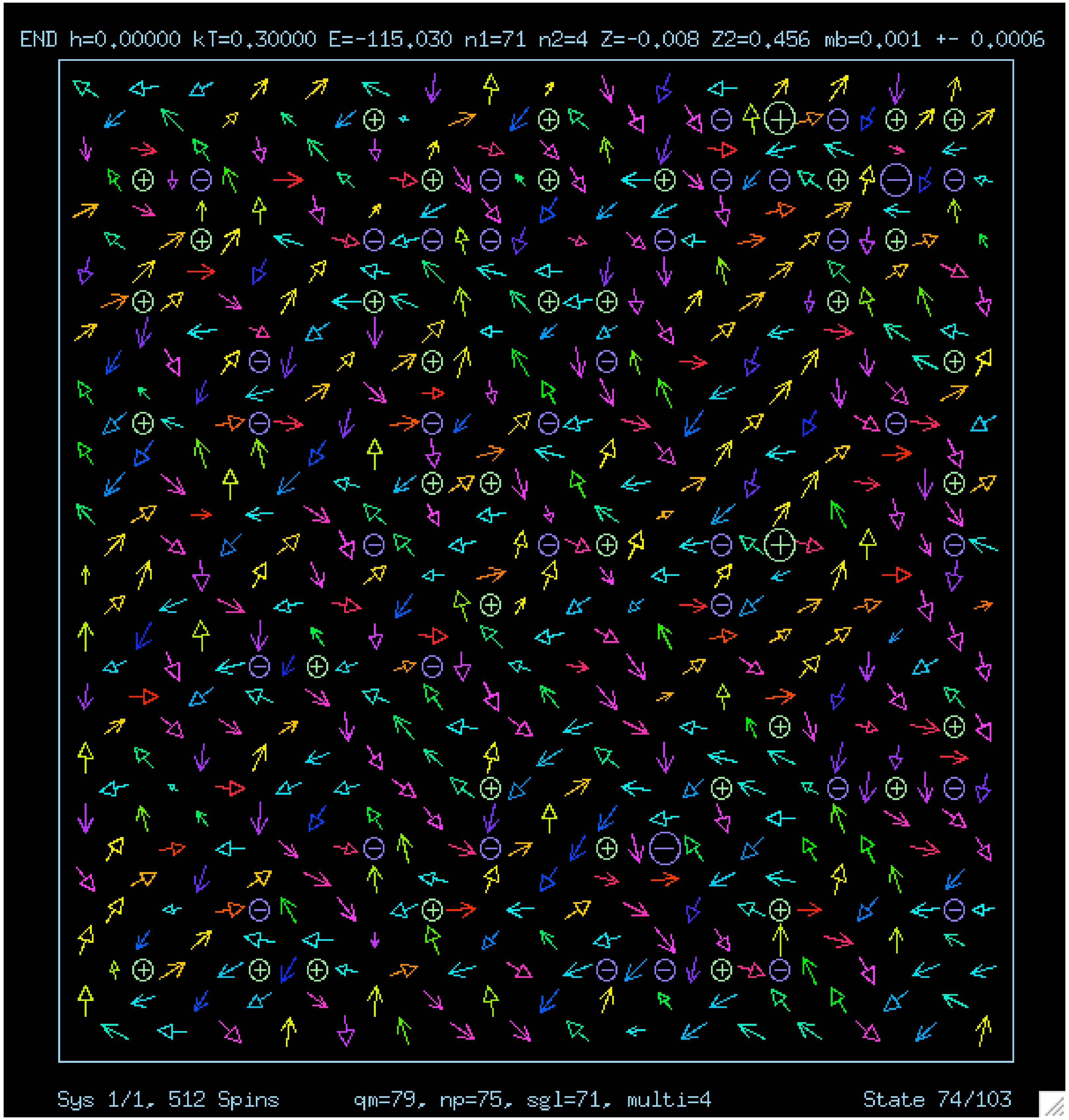

$D = 0.1$

$K_1=0.1$

$K_3=0.5$

$kT=0.30$

$\approx$ high-T disorder

(from long-time Langevin dynamics)

ice model for Wang et al (2006) particles

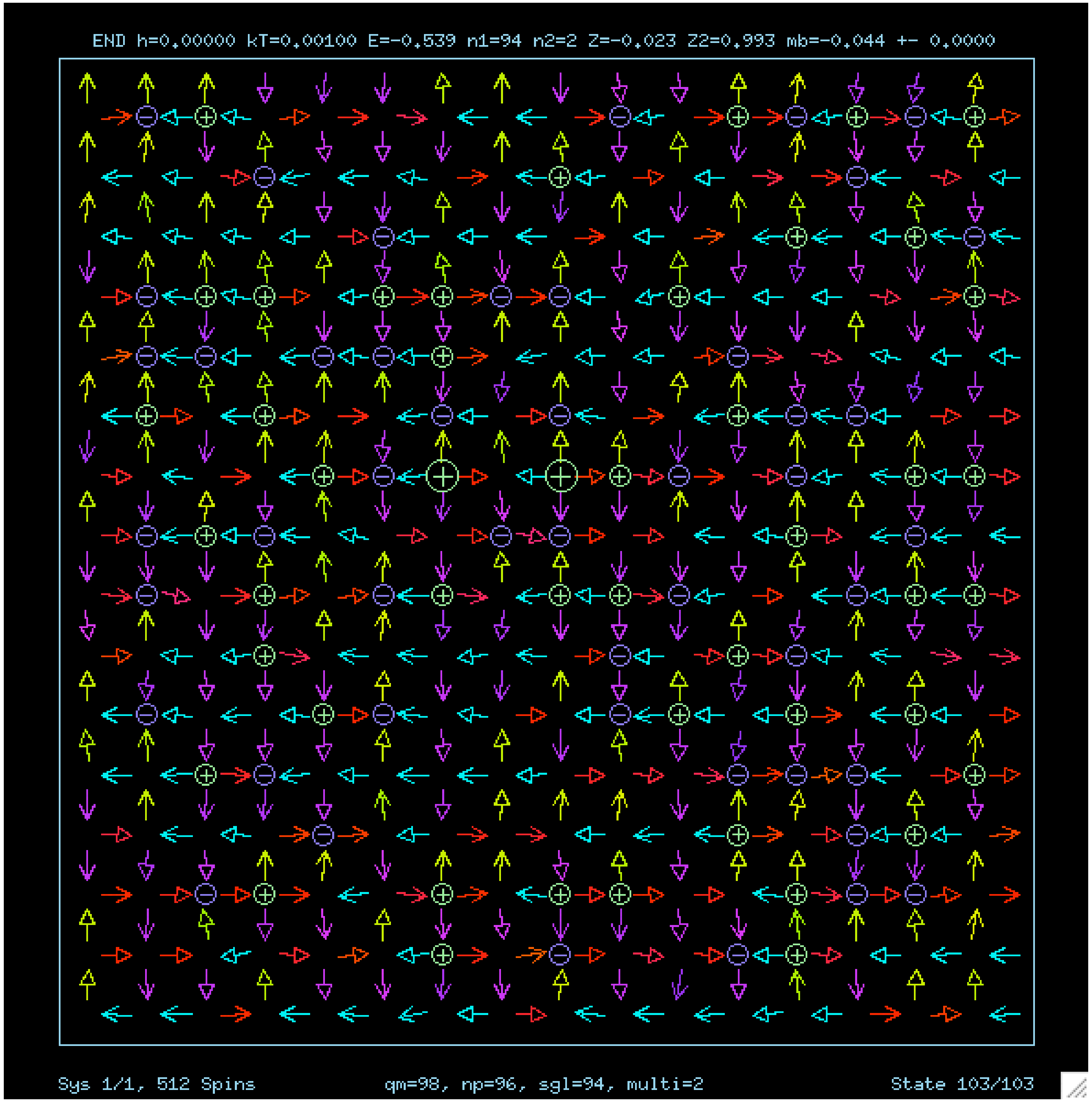

$D = 0.000835$
$K_1 = 0.0897$
$K_3 = 0.2000$

$kT = 0.001$

$\neq$ ground state

(from long-time Langevin dynamics)

Note: 300 K is $kT = 1.29 \times 10^{-5}$

$$D = \frac{\mu_0}{4\pi} \frac{\mu^2}{a^3}$$

ice model for Wang et al (2006) particles

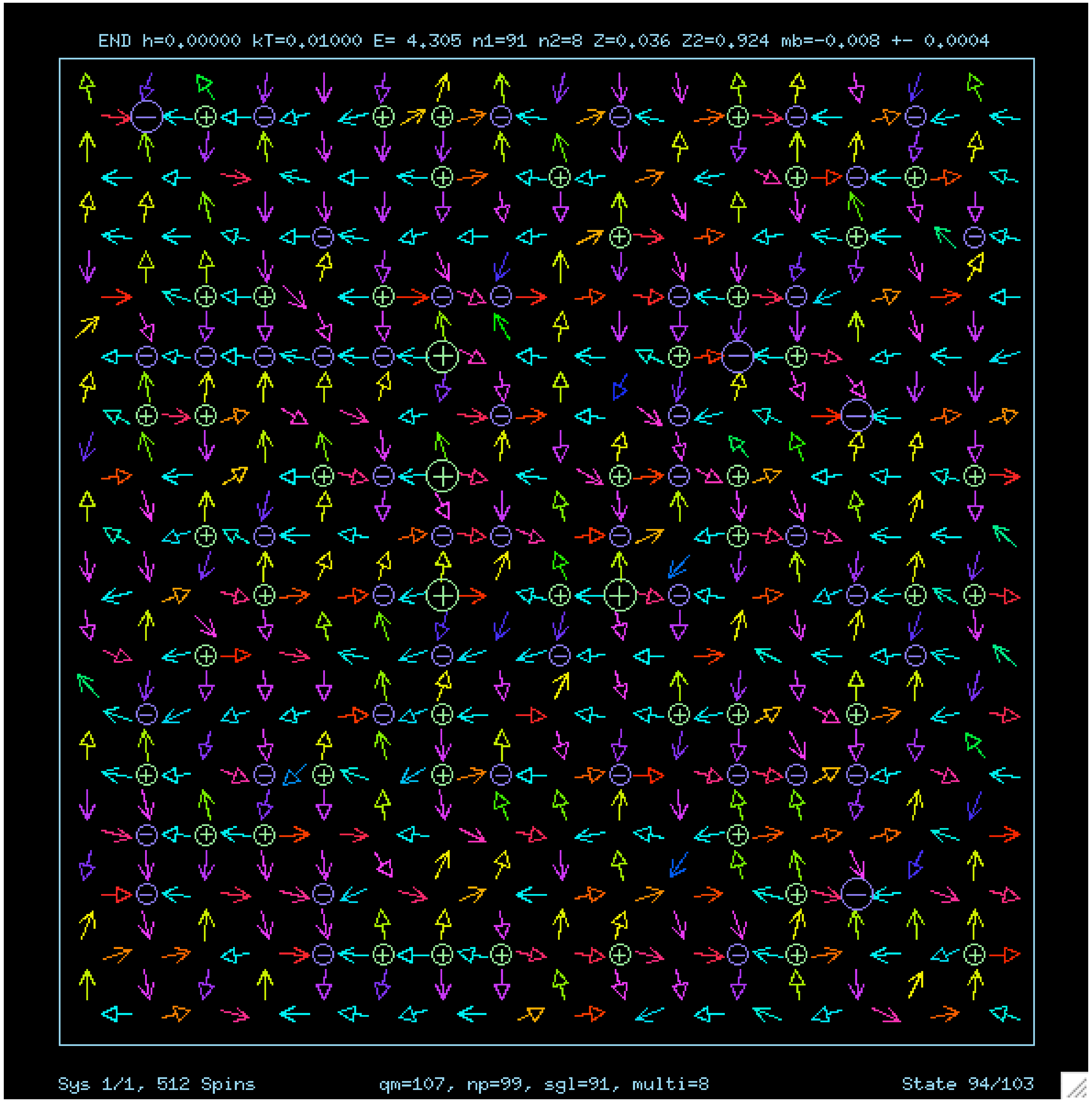

$D = 0.000835$

K_1=0.0897

K_3=0.2000

kT=0.01

$\neq$ ground state

(from long-time Langevin dynamics)

ice model for Wang et al (2006) particles

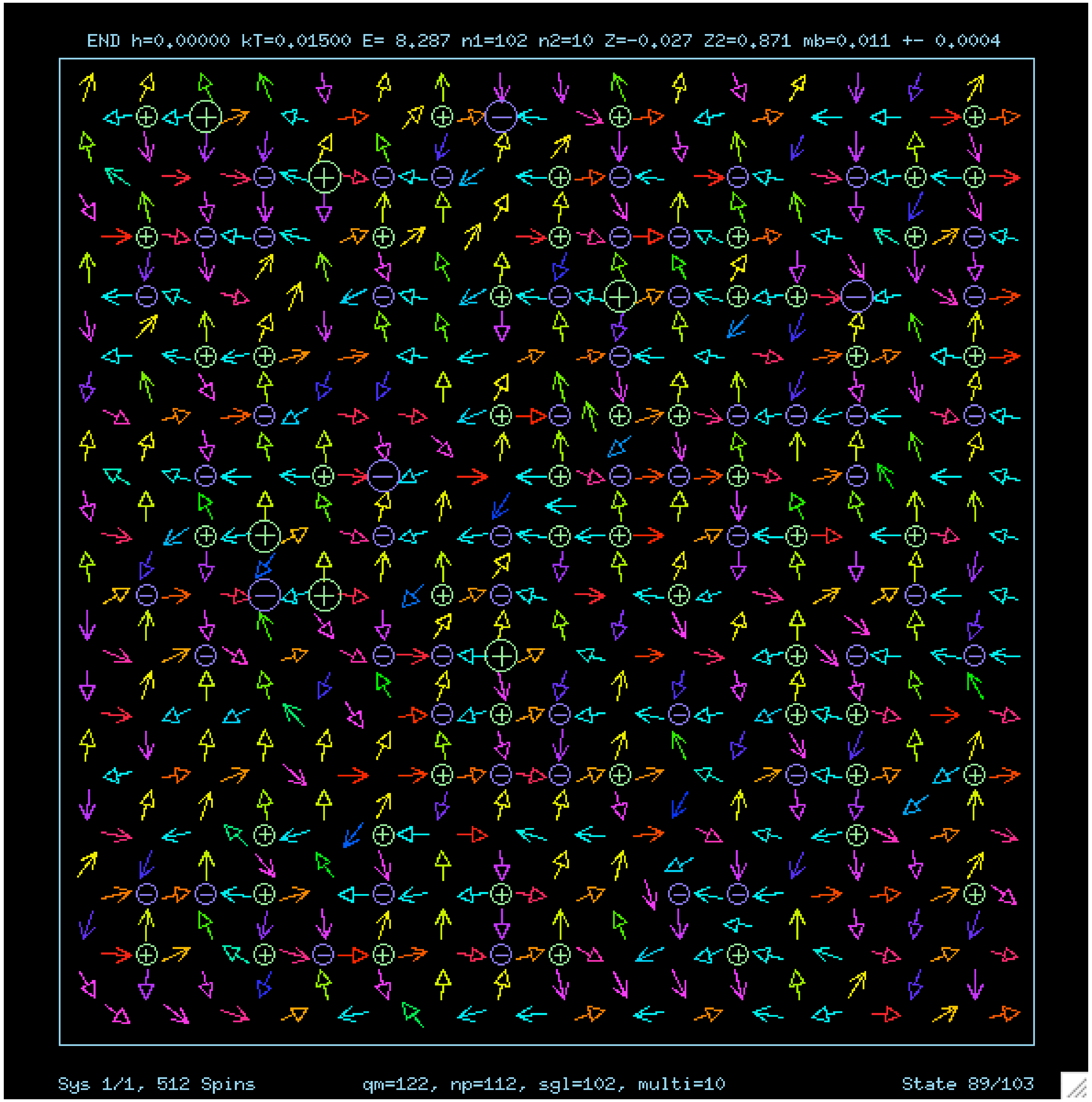

$D = 0.000835$

$K_1=0.0897$

$K_3=0.2000$

$kT=0.015$

more monopoles

(from long-time Langevin dynamics)

ice model for Wang et al (2006) particles

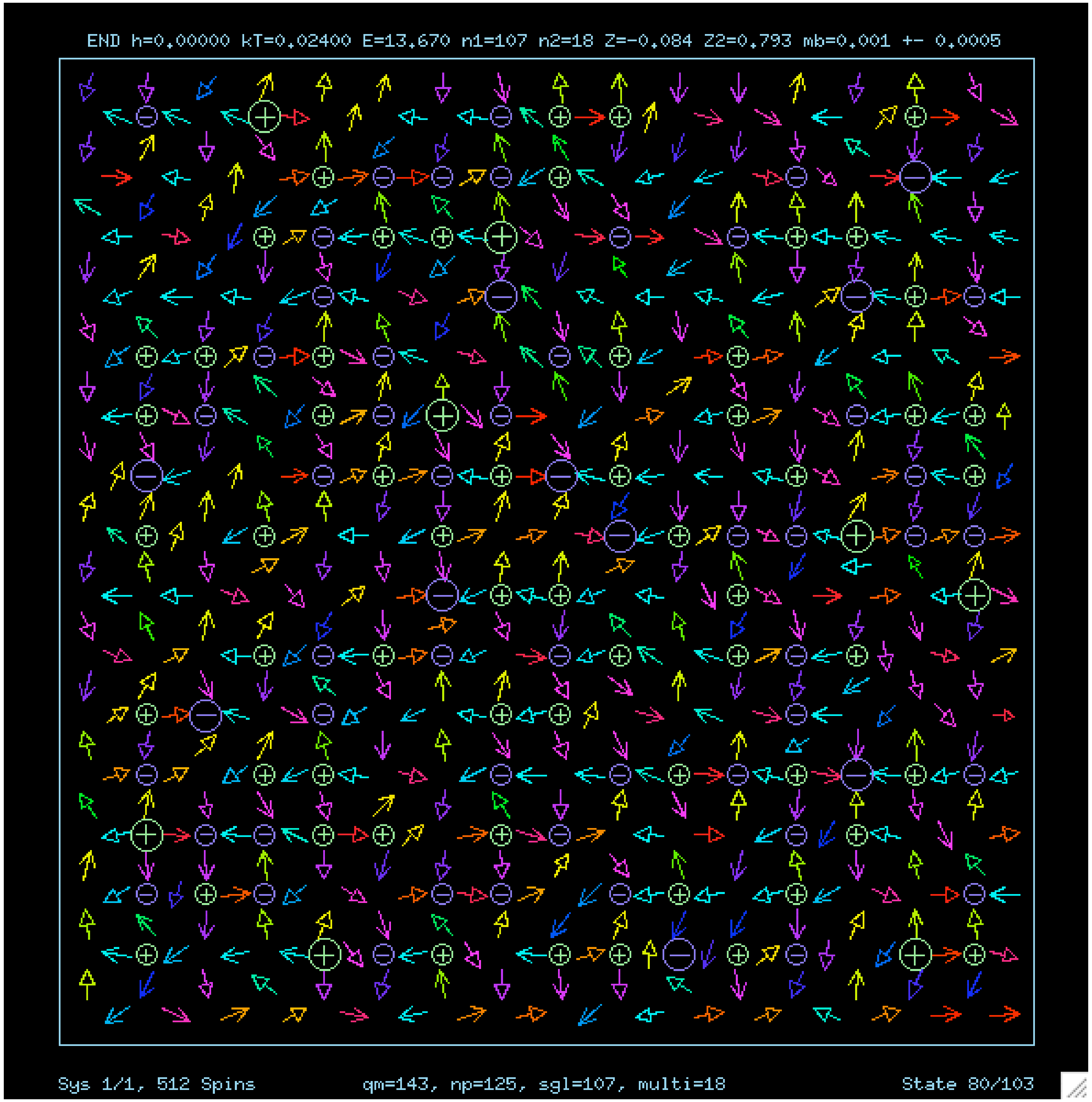

$D = 0.000835$

$K_1=0.0897$

$K_3=0.2000$

$kT=0.024$

more monopoles

(from long-time Langevin dynamics)

ice model for Wang et al (2006) particles

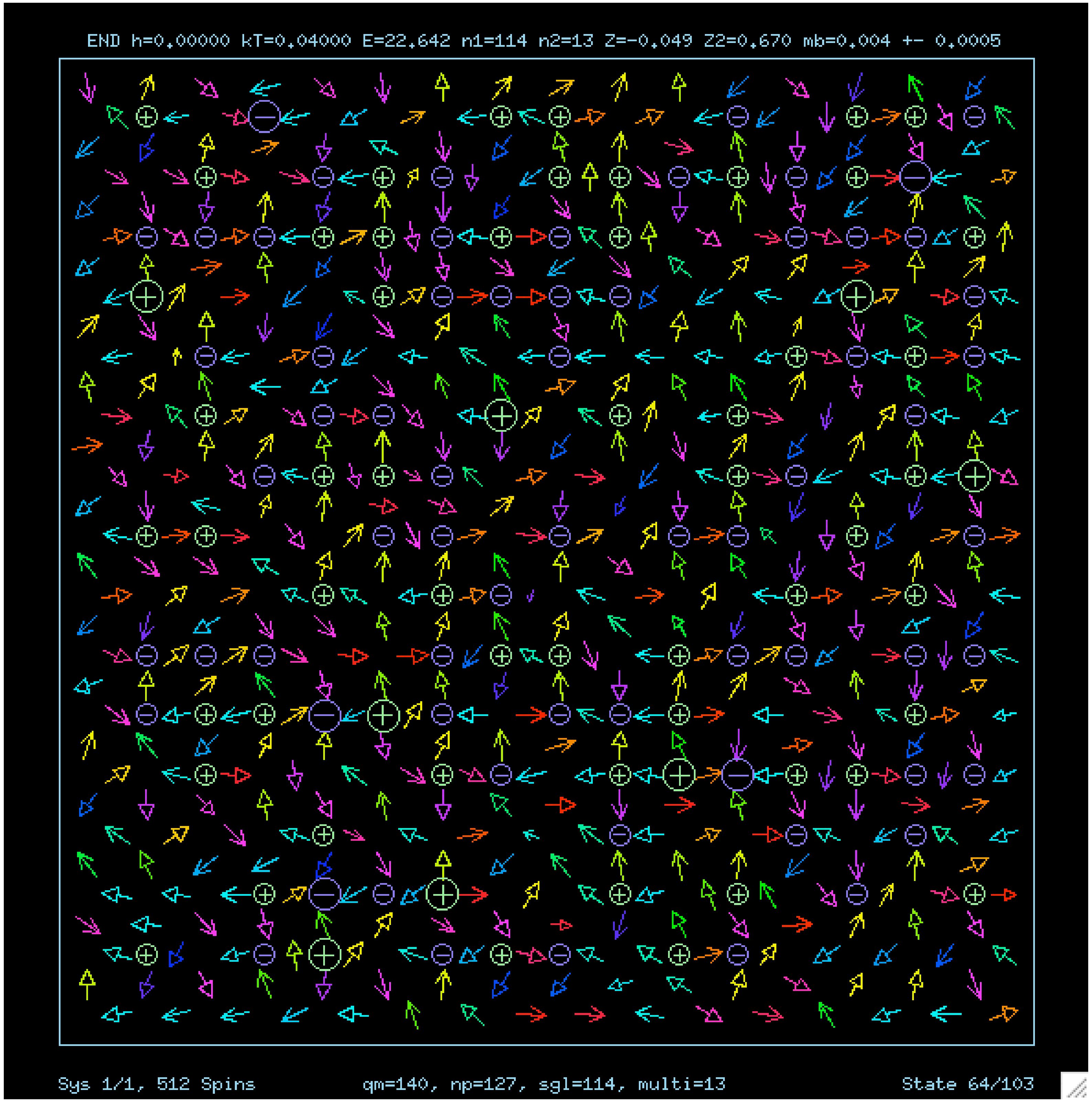

$D = 0.000835$
K_1=0.0897
K_3=0.2000

kT=0.040

highly disordered

(from long-time Langevin dynamics)

artificial ice model - Kagomé lattice

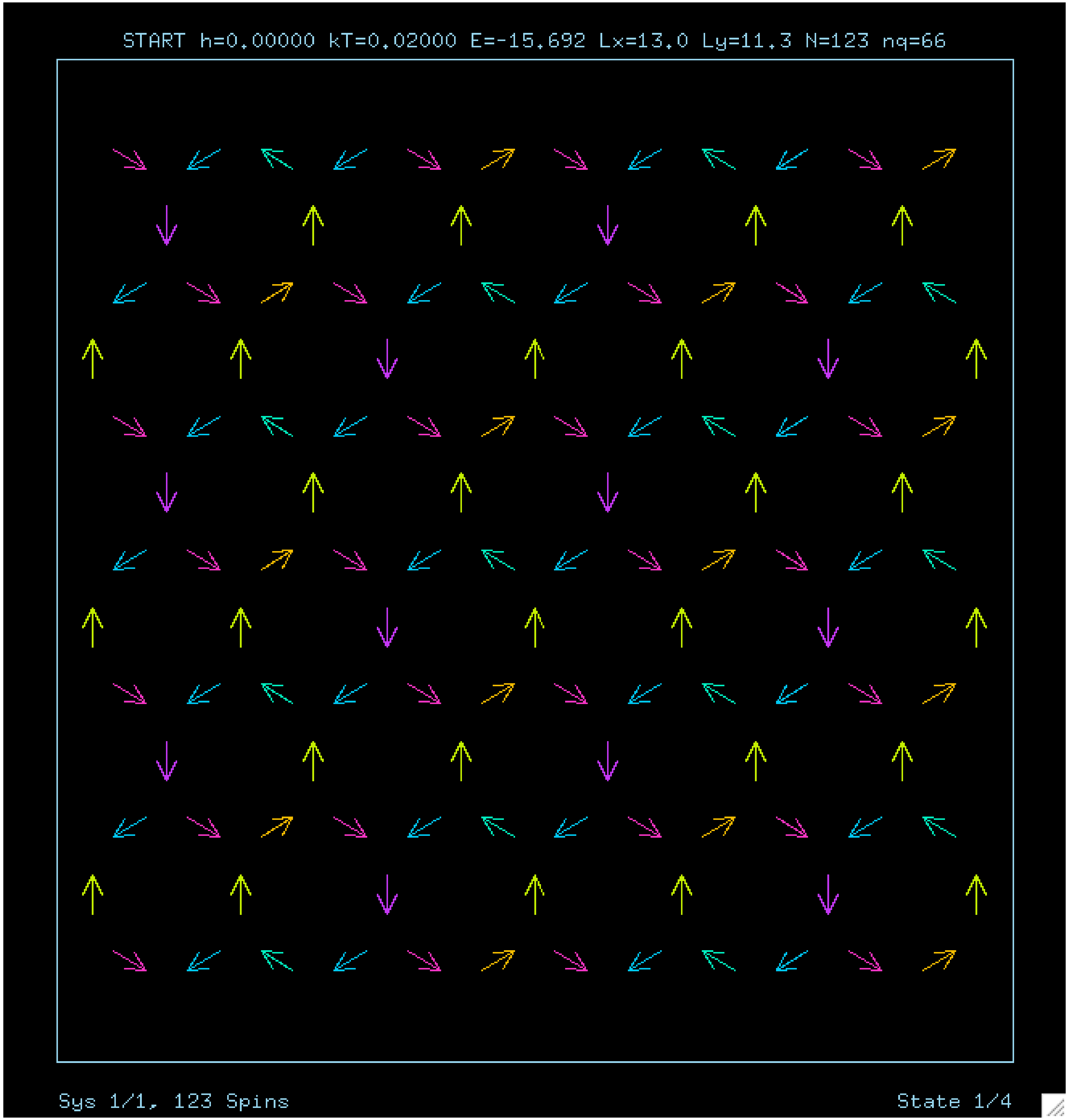

D = 0.1

K_1=0.1

K_3=0.5

1 of 6
ground states

artificial ice model - Kagomé lattice

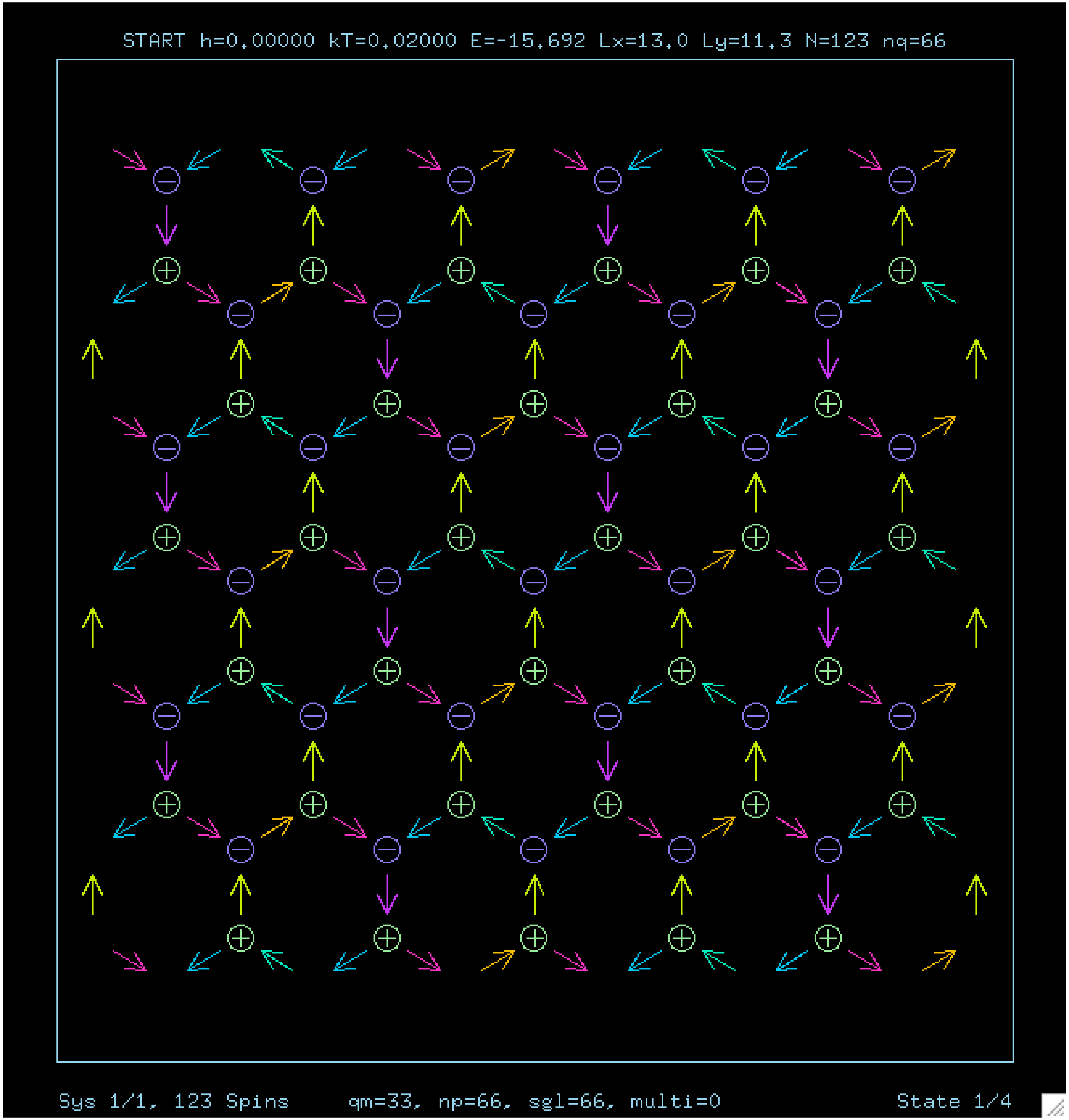

D = 0.1
K_1=0.1
K_3=0.5

1 of 6
ground states

all vertices have a monopole charge.

artificial ice model - Kagomé lattice

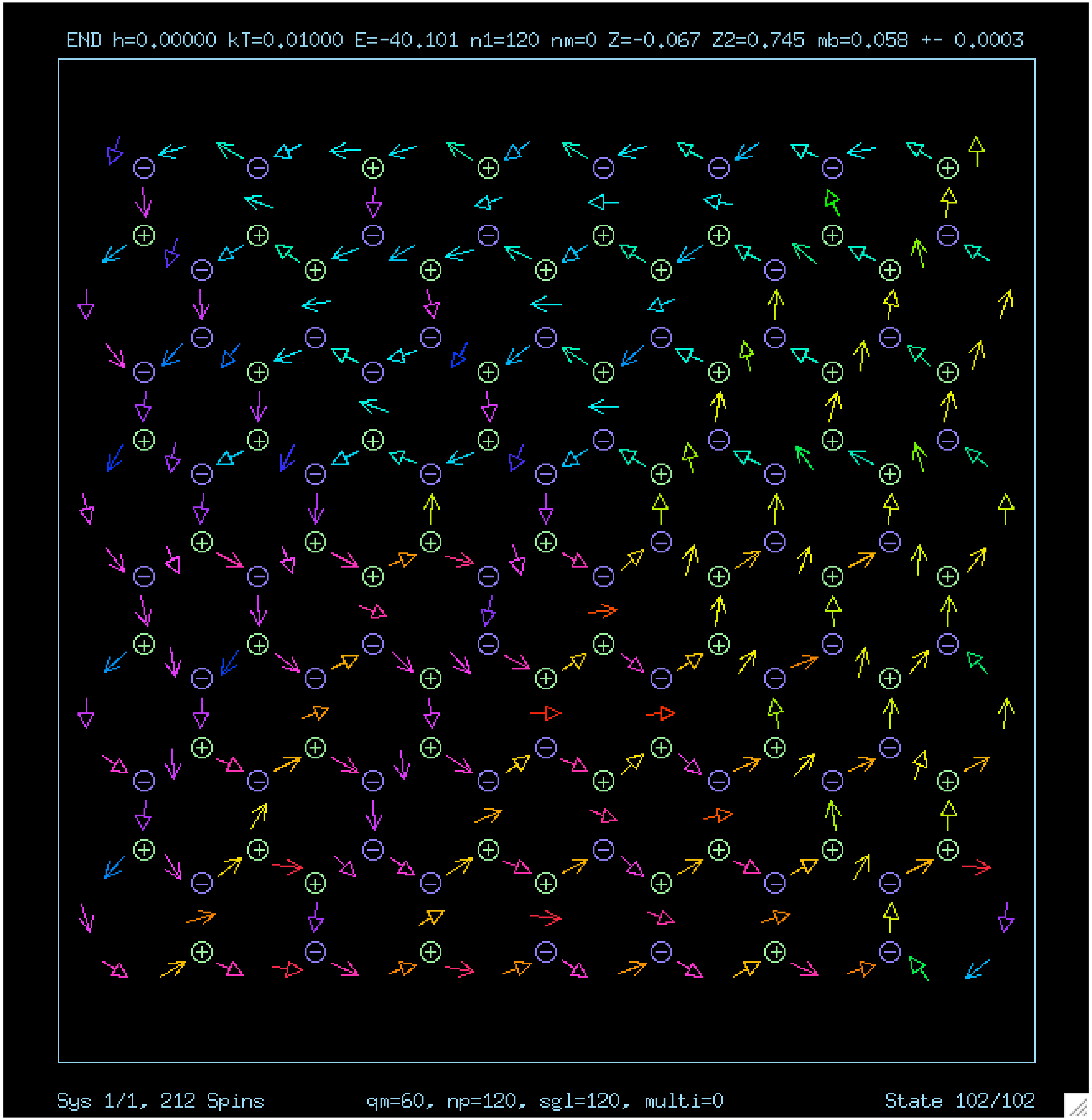

$D = 0.1$

$K_1=0.1$

$K_3=0.5$

$kT=0.01$ (low T).

Frustrated state does not approach ground state.

(from long-time Langevin dynamics)

artificial ice model - Kagomé lattice

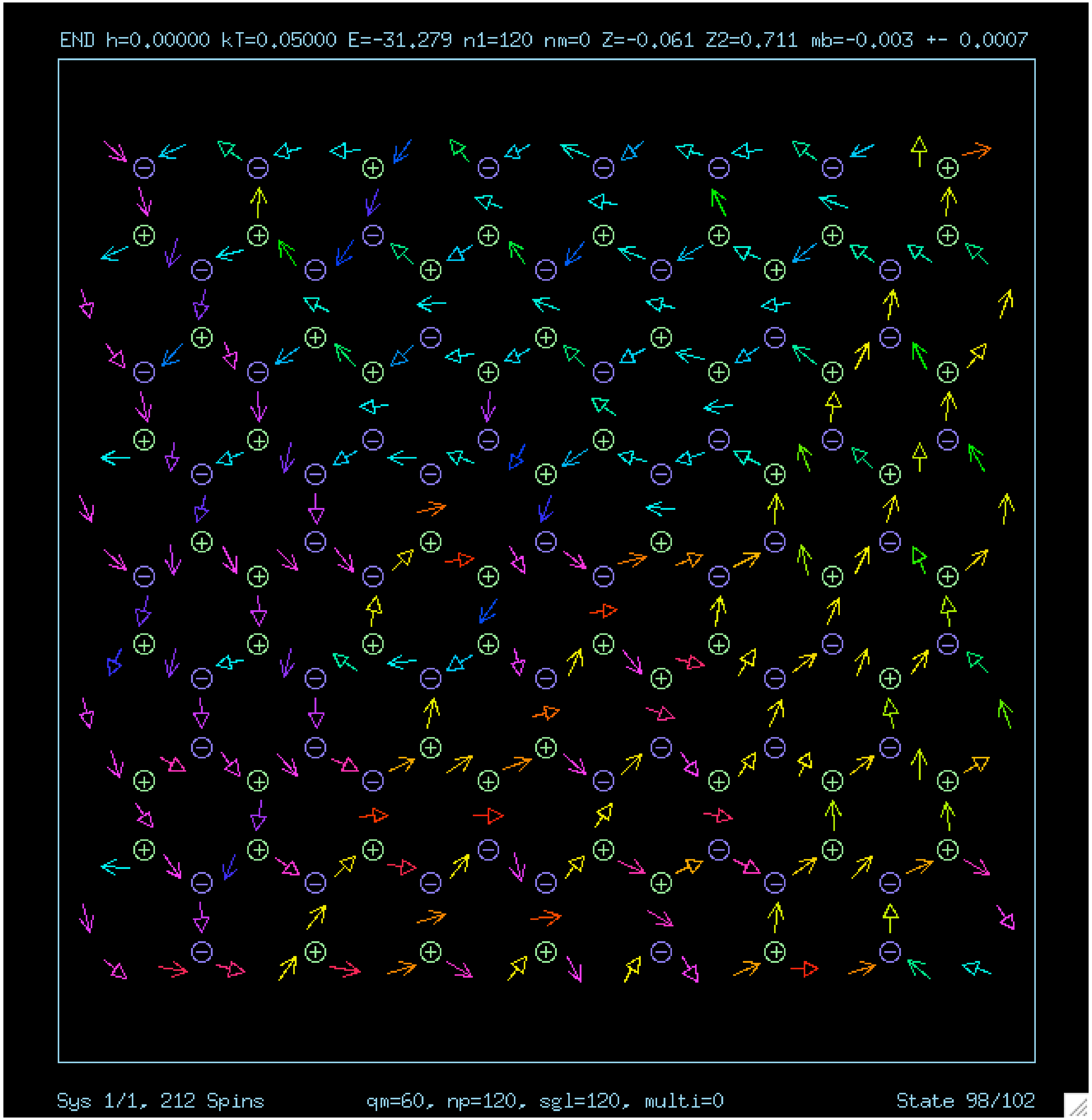

$D = 0.1$

$K_1=0.1$

$K_3=0.5$

$kT=0.05$

(from long-time Langevin dynamics)

artificial ice model - Kagomé lattice

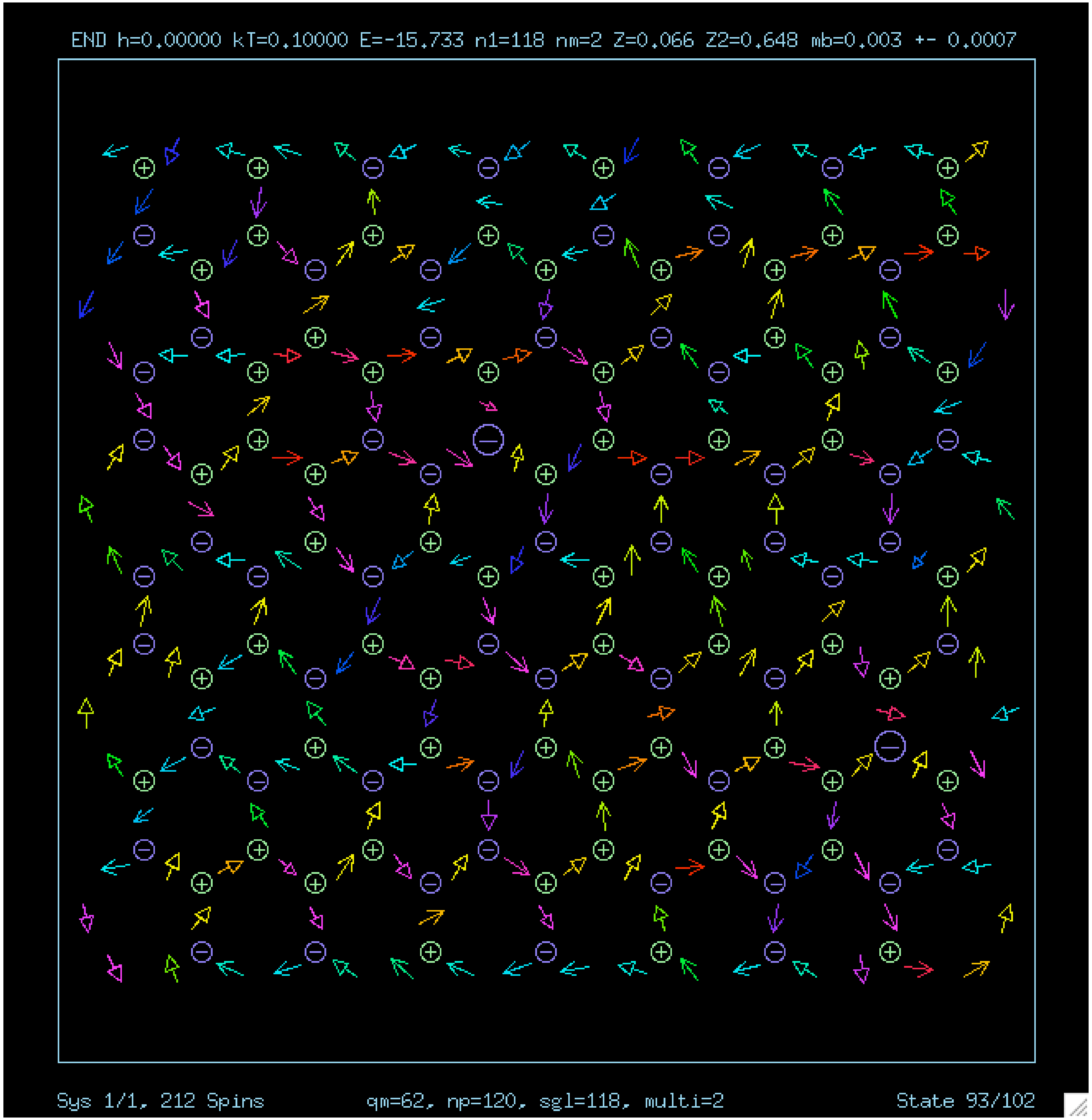

$D = 0.1$

$K_1=0.1$

$K_3=0.5$

$kT=0.1$ (moderate)

multi-charge poles

(from long-time Langevin dynamics)

artificial ice model - Kagomé lattice

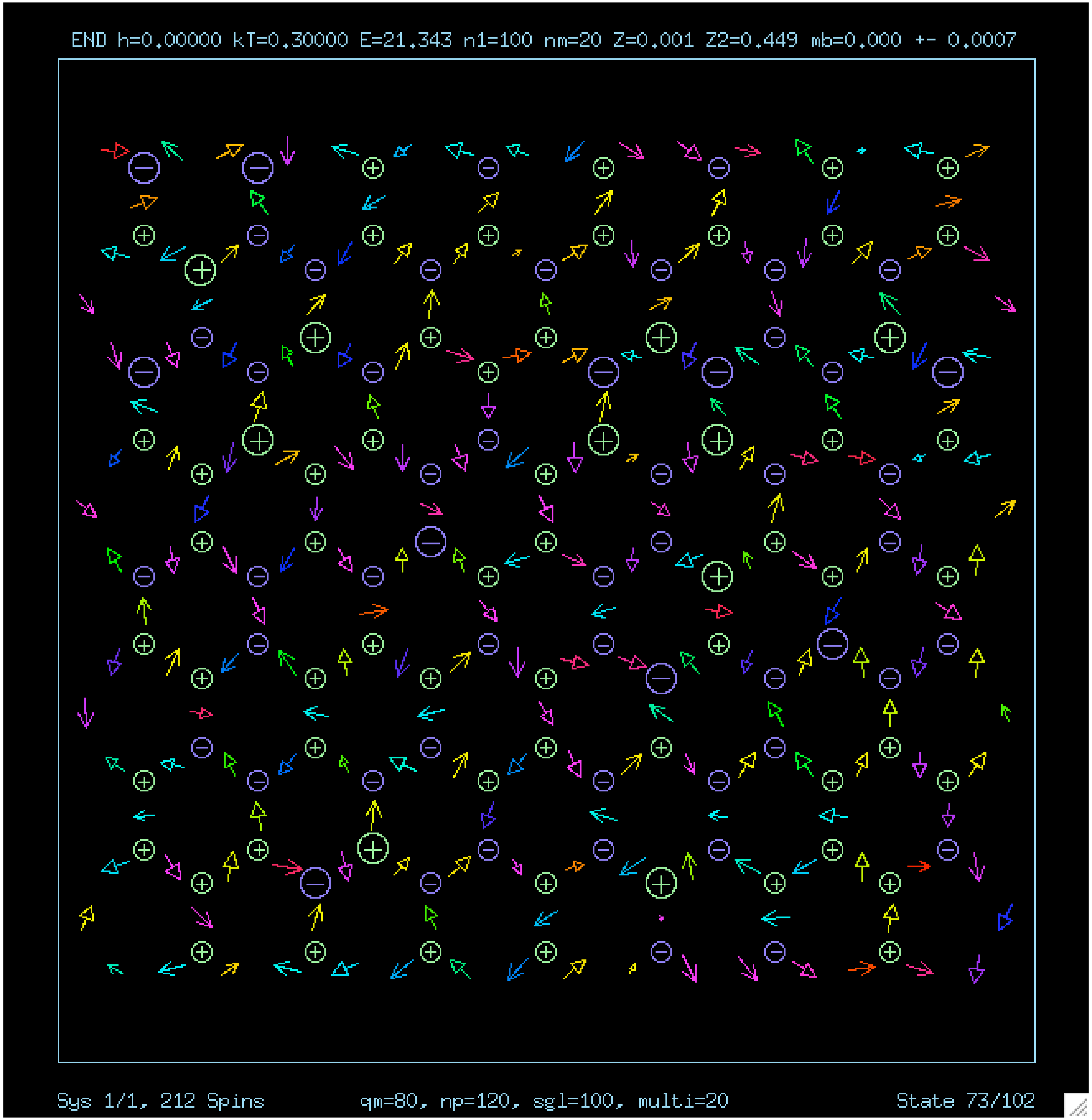

$D = 0.1$

$K_1=0.1$

$K_3=0.5$

$kT=0.3$ (high)

many
multi-charge poles

(from long-time
Langevin dynamics)

Summary

Shape anisotropy of magnetic islands has a strong effect on the states.

Vortices in nanodots have frequency ω_G of gyrotropic movement, which is proportional to the force constant over thicknes, k_F/L.

Even thermal fluctuations can initiate spontaneous vortex motion that satisfies equipartition of energy.

Anisotropy coefficients for islands used in artificial spin ice are found from the effective potential of the magnetic moment in an island.

A model is developed for spin-ice, based on effective island dipoles which can point in any direction, but constrained by anisotropies.

wysin@phys.ksu.edu
www.phys.ksu.edu/personal/wysin